MJHI | Moroccan Journal of Health and Innovation

VOLUME 1
ISSUE N° 2
JULY
2025

Moroccan Journal of Health and Innovation

DÉPÔT LÉGAL : 2025PE0023 | E-ISSN: 3085-5047
www.mjhi-smb.com | smbmjhi@gmail.com

SMB الجمعية المغربية البيوطبية SOCIÉTÉ MAROCAINE BIOMÉDICALE | ICBES INTERNATIONAL CONFERENCE ON BIOMEDICAL ENGINEERING AND SCIENCE

Editors and Reviewers Information

ISSN 2025PE0023 (paper version) ISSN 3085-5047 (electronic version)

https://mjhi-smb.com

Editorial: Precision, Progress, and the Future of Medicine

Moroccan Journal of Health and Innovation (MJHI) – Volume 1, No 2

The Moroccan Journal of Health and Innovation (MJHI), a scientific platform that emerged from the 3rd International Conference on Biomedical Engineering and Science (ICBES), which took place during the 4th Rencontre Biomédicale (RMB) of the Moroccan Biomedical Society (SMB) in Marrakech from February 20 to 22, 2025, is pleased to present its second issue of Volume 1.

The multidisciplinary convergence of clinical technology evaluation, artificial intelligence, and biological innovation fields that are altering the parameters of contemporary healthcare is reflected in this issue. The five chosen articles provide an engaging look at Morocco's and other countries' ever-changing research environment.

A very unique work on three-dimensional human hearing modeling using the finite element approach opens the issue. The authors replicate the mechanical behavior of the auditory system by integrating bone, cartilage, skin, and the tympanic membrane, going beyond traditional models. In addition to advancing anatomical teaching, this study establishes the foundation for upcoming biomechanical and audiological applications.

Two papers explore how artificial intelligence is affecting medical imaging, with a focus on deep learning's diagnostic potential. A cutting-edge analysis of generative AI methods, including diffusion models, GANs, and VAEs, applied to cardiac MRI is the first. This study demonstrates how the lack of annotated datasets can be addressed and how improving diagnostic precision in cardiology—still the leading cause of death worldwide may be achieved through the creation of synthetic data.

The use of deep learning, particularly convolutional neural networks (CNNs), in the detection of brain tumors is reviewed in the second AI-focused contribution. The authors evaluate the effectiveness of several CNN models across multiple imaging modalities and datasets by conducting a thorough evaluation of studies conducted between 2020 and 2024. Their results highlight the advancements as well as the remaining obstacles in the pursuit of accurate, real-time tumor identification.

An empirical assessment of CNN's performance in medical picture categorization is included in a different publication to supplement this review. The work validates the reliability of CNNs as instruments to assist clinical decision-making, particularly in environments with limited resources, by assessing the models' accuracy and loss during multiple training epochs.

The issue concludes with a critical analysis of the accuracy of glucometers that are often used in Morocco. The authors compare the readings from these devices to those from a recognized laboratory after testing them under various biological interferences. Despite frequently overestimating blood glucose levels by 22%, the glucometers maintained a strong correlation with laboratory data ($r = 0.95$), confirming their usefulness for glycemic monitoring—as long as calibration standards are strengthened before being distributed.

When taken as a whole, these contributions show a thriving ecosystem of research where local problems lead to internationally applicable answers and where technology advances both science and medical care. Inspiring academics, clinicians, and innovators to pursue cooperative, significant work in health and biomedical science is our goal with this issue of MJHI.

We would like to thank all of the authors, reviewers, and conference attendees for their hard work and priceless input. With every issue of MJHI, which has only just begun, we renew our dedication to promoting scientific quality, encouraging innovation, and elevating Moroccan research internationally.

Pr. Dr. Hicham CHATOUI

Editor-in-Chief & Publication Director

Moroccan Journal of Health and Innovation (MJHI)

Table of Contents

MJHI | Moroccan Journal of Health and Innovation

Article N°1, Vol 1, No 2

Deep Learning Approaches to Brain tumor Detection: A Review

Amal Kaab [1], Zakaria Hachkar [2], Younes Chihab [3]

1 Physics, Energy, Environment and Applications Laboratory (LP2EA), Cadi Ayyad University, Polydisciplinary Faculty of Safi, Moroccoamalkaab97@gmail.com
2 Physics, Energy, Environment and Applications Laboratory (LP2EA), Cadi Ayyad University, Polydisciplinary Faculty of Safi, Morocco
3 Computer Science Research Laboratory (LaRI), Faculty of Sciences, Ibn Tofail University, Kenitra, Morocco.
* amalkaab97@gmail.com

Abstract: Brain tumors are a major global health challenge and one of the leading causes of death worldwide. Early detection is critical to improving survival. However, obtaining reliable and accurate results remains a significant challenge, even when utilizing high-quality brain imaging techniques. Diagnosing a brain tumor is often a lengthy process that requires extensive radiological expertise. In this context, using deep learning, particularly convolutional neural networks (CNNs), is a promising approach for improving both the accuracy and the efficiency of the diagnosis of brain tumors. This review analyses studies published between 2020 and 2024 on deep learning techniques to identify and categorize brain tumors. It also highlights the variety of methodologies and algorithms that have been put forth and evaluates the diverse applications of deep learning. In addition to publicly available datasets, it examines radiological imaging techniques. The aim of this study is to evaluate the effectiveness of different deep learning models in the identification and categorization of brain tumors from medical scans. Furthermore, the review highlights notable advances in the field and underscores crucial gaps.

Keywords: medical imaging, brain tumor detection, convolutional neural networks, deep learning.

Received: April 13, 2025
Revised: May 20, 2025
Accepted: June 05, 2025
Published: July 25, 2025

Citation: Kaab, A.; Hachkar, Z.; Chihab, Y. Deep Learning Approaches to Brain tumor Detection: A Review. Moroccan Journal of Health and Innovation (MJHI) 2025, Vol 1, No 2. https://mjhi-smb.com

1. Introduction

Brain tumors are a major global health problem, accounting for more than 300,000 cases each year, according to the World Health Organization (WHO). They have increasing incidence rates worldwide (Arulmani et al., 2024). This makes early diagnosis a necessity to prevent their prevalence. Machine learning and deep learning can help diagnose and prevent brain tumors. Deep learning algorithms are the most preferred due to their high performance.

Brain tumors can be divided into two main categories (Arulmani et al., 2024): primary tumors, formed in the brain, and metastatic tumors, originating in other parts of the body and four times more frequent. Primary tumors are either glial or non-glial, benign or malignant. The WHO has classified tumors into 4 grades according to their malignancy, growth and histological characteristics. Grade 1 tumors are benign, growing slowly and often treatable by surgery. Grade 2 tumors, though benign, may involve neighboring tissues and recur at a higher grade. Grade 3 tumors, which are malignant, propagate rapidly and require treatments such as chemotherapy. Grade 4 tumors, the most aggressive, spread rapidly, recur frequently and require combined therapies.

Brain tumors can be classified according to how they grade, as follows (Kim and Lee, 2022): Craniopharyngiomas, which are benign but difficult to remove because of their proximity to critical structures such as the pituitary gland, are a type of low-grade brain tumor (grades I and II). Chordomas, rare malignancies, typically affect the axial bones and require targeted radiation therapies such as carbon ion or proton therapy. Gangliogliomas and gangliocytomas, often associated with seizures, develop in the temporal lobes and are common in young adults. Schwannomas, benign tumors of the peripheral nerves, are often treated with surgery or radiation, although vestibular schwannomas can cause hearing loss. Pituitary adenomas and pineocytomas, which are usually benign, occur in the pituitary gland and pineal gland, respectively, and are generally slow growing and treatable. High-grade (grade III and IV) brain tumors include anaplastic astrocytomas, aggressive malignancies that require surgery, radiation therapy, and chemotherapy. Anaplastic oligodendrogliomas, which originate from myelin-producing cells, also require a multimodal approach. Glioblastoma multiforme (GBM), the most malignant and aggressive form, is distinguished by abnormal cells, necrotic areas, and new blood vessel formation. There is no standard treatment for recurrent cases, but treatment typically includes surgery, radiation and chemotherapy.

The World Health Organization (WHO) classified malignant brain tumors as destructive and fatal neoplasms with high mortality rates that affect all age groups (Xie et al., 2022). According to the WHO, 9.6 million people worldwide die from brain tumors each year. Brain tumors are a common and serious disease that significantly reduces the life expectancy of people of all genders and all age

groups (Buabeng et al., 2024). Early detection and treatment are critical to prevent permanent organ damage.

In the field of medical decision support, artificial intelligence (AI) is increasingly being used for disease detection and accurate diagnosis, has made remarkable progress in recent years. Solving real-world problems in different fields. Deep learning (DL), a branch of AI, is rapidly revolutionizing several fields by successfully tackling complex challenges like natural language processing and image recognition. Its powerful capabilities have also been applied to medicine, where DL models have proven effective in a variety of applications.

This paper is structured as follows: Section 2 presents an overview of machine learning and deep learning techniques used for brain tumor classification and detection. Section 3 discusses different imaging modalities, datasets and selection criteria considered in this review. Section 4 provides a performance analysis, while Section 5 concludes the study.

2. Literature review of brain tumor classification models

A wide range of machine learning and deep learning methods have been developed for brain tumor image classification. In (Prabha and Singh, 2024), the authors used the EfficientNet family to automatically detect and classify three types of brain tumors using magnetic resonance imaging (MRI). Their study demonstrated the effectiveness of these architectures, achieving the following accuracy rates 96.07% (EfficientNet-B0), 97.86% (EfficientNet-B1), 98.21% (EfficientNet-B2), 97.86% (EfficientNet-B3), 98.93% (EfficientNet-B4), 99.64% (EfficientNet-B5), 98.57% (EfficientNet-B6) and 99.64% (EfficientNet-B7).

In (Tiwari et al., 2025), Raj Gaurang Tiwari et al. introduced the Adaptive Neuro-Fuzzy Inference System-Fusion-Deep Belief Network (ANFIS-F-DBN) model, which achieved an accuracy of 90.00%. In [13], the authors propose an automatic brain tumor diagnosis system that uses a convolutional neural network (CNN) for both classification and segmentation of glioblastomas. Using 1,800 images from the BraTS 2017 dataset, their model achieved a maximum accuracy of 99%.

The study in (Ahmed et al., 2024) introduced a hybrid ViT-GRU model, where the Vision Transformer (ViT) extracts essential features and the Gated Recurrent Unit (GRU) identifies relationships between them. This approach effectively addresses class imbalance and outperforms existing diagnostic methods. The model was trained using multiple optimizers, including SGD, Adam and AdamW, and evaluated through rigorous 10-fold cross-validation. In addition, Explainable Artificial Intelligence (XAI) techniques - such as Attention Maps, SHAP and LIME - were integrated to improve interpretability. On the primary data set, BrTMHD-2023, the model achieved its highest accuracies with different optimisers: 81.66% (SGD), 96.56% (Adam) and 98.97% (AdamW). In

(Alshuhail et al., 2024), the authors developed a deep learning based model using convolutional neural networks (CNNs). The proposed model follows a sequential CNN architecture with multiple convolutional, max-pooling and dropout layers followed by dense layers. This model achieved an overall test accuracy of 98%, demonstrating a significant improvement in diagnostic accuracy.

Suganya Athisayamani et al (Alshuhail et al., 2025) used the AlexNet50 deep model for classification using a discriminative learning method. Their approach consists of three learning stages: (1) feature learning using the entire dataset, (2) training on an extended dataset while freezing certain AlexNet50 layers, and (3) further training on the extended dataset while leaving the frozen layers unchanged. The method was tested on three publicly available MRI classification datasets. Several hyperparameter optimisation techniques - including Adam, Stochastic Gradient Descent (SGD), Root Mean Square Propagation (RMSprop), Adamax and AdamW - were used to evaluate the learning process. The highest classification performance was achieved on the HWBA dataset with an average accuracy of 98%.

In 2024, researchers have proposed a novel MRI-based brain tumor detection method that integrates machine learning and deep learning techniques. MRI images were pre-processed using a median filter combined with an adaptive contrast enhancement algorithm (ACEA) to improve image quality and reduce noise. Segmentation was performed using a fuzzy c-means algorithm. Feature extraction was based on the grey level co-occurrence matrix (GLCM), including energy, mean, entropy and contrast. Classification was performed using the Ensemble Deep Neural Support Vector Machine (EDN-SVM), which combines deep neural networks with SVMs. The model achieved 97.93% accuracy in distinguishing between normal and abnormal brain tissue in MRI scans (Anantharajan et al., 2024). Zelenak and collaborators have introduced the Brain Tumor Recognition using an Equilibrium Optimizer with a Deep Learning Approach (BTR-EODLA) technique for MRI image analysis. This method is designed for high accuracy brain tumor detection. The BTR-EODLA approach applies median filtering (MF) to reduce noise in MRI scans, uses the squeeze-excitation ResNet (SE-ResNet50) model for feature extraction, and uses the Equilibrium Optimizer (EO) to fine-tune model parameters. A Stacked Autoencoder (SAE) is then used for tumor detection. Experimental results showed an impressive accuracy of 98.78%, confirming the effectiveness of the proposed technique (Zelenak et al., 2013).

3. Méthodologie

In this section, we present the criteria taken into account when selecting the papers chosen in the present work, as well as different brain tumor detection datasets and medical imaging techniques.

3.1. Selection criteria

The articles selected for this paper were searched using databases known for their coverage of medical and deep learning related scientific publications. Specifically, we used PubMed, Google Scholar and Scopus, which highlights the most recent and relevant research in medical imaging and artificial intelligence. It includes only studies published between 2021 and 2025 that focus on leveraging deep learning techniques for brain tumor detection and classification. Inclusion criteria were strictly defined and included papers that applied deep learning models to medical images, including MRI and PET scans.

3.2. Medical imaging techniques and datasets

3.2.1. Medical imaging techniques

A number of conventional methods have been used in the past for brain tumor imaging (Zelenak et al., 2013), these include non-invasive and invasive imaging modalities such as x-rays, ultrasound, computed tomography (CT) and magnetic resonance imaging (MRI). While X-rays played a pivotal role in their early use, their low sensitivity led to the subsequent emergence of more advanced techniques, such as CT and MRI. Ultrasound continues to find application in real-time intraoperative monitoring, but its use has been largely supplanted by MRI-based neuronavigation. The use of CT is effective in the detection of bone abnormalities and provides rapid imaging; furthermore, advanced techniques such as CT angiography and perfusion imaging are now well established. MRI is considered the gold standard in brain imaging; its unparalleled tissue contrast and detailed imaging make it ideal for tumor assessment. However, it should be noted that CT is more widespread and affordable than MRI.

3.2.2. Datasets

Researchers have used several MRI datasets for brain tumor classification. These include the Brain Tumor Dataset (from Figshare or collected by the authors), the BRATS Dataset (especially BRATS2015), and datasets available on Kaggle. These databases typically include classes such as meningioma, glioma, pituitary, or tumor/non-tumor. MRI scans are often pre-processed (e.g. resized, normalized, noise suppressed) before analysis. Researchers can collect data directly or get it from public databases (like Figshare) and use it to classify images into categories of binary (tumor/non-tumor) or multi-class (specific tumor types). Table 1 summarizes the dataset types used in the studies included in this review.

Table 1. datasets used in brain tumor classification.

Dataset	Source	Classes
Brain Tumor Dataset	Figshare, Collected by authors	Meningioma, Glioma, Pituitary, Tumor / Non-Tumor
BRATS Dataset	BRATS2015	High Grade Glioma, Low Grade Glioma
Figshare Dataset	Figshare	Meningioma, Glioma, Pituitary, Tumor / Non-Tumor
Kaggle Dataset	Kaggle	Cancerous, non-cancerous
MRI Images Collected	By authors	Glioma, Meningioma, Pituitary, Tumor / Non-Tumor
Brain MRI Images	Various sources	Tumor / non-tumor

4. Performance analysis

Several methods stand out for their high accuracy, among the most effective approaches for brain tumor classification. The EfficientNet family (Prabha and Singh, 2024), using the EfficientNet-B5 and B7 architectures, reached a maximum accuracy of 99.64%, demonstrating the effectiveness of these models in MRI image analysis. The hybrid ViT-GRU model (Ahmed et al., 2024) achieved outstanding results, reaching an accuracy of 98.97% through the integration of explicable AI techniques and hyper-parameter optimization. Using classical architectures, AlexNet50 (Alshuhail et al., 2025) and a sequential CNN model (Alshuhail et al., 2024) both achieved 98.00% accuracy. Another promising method, the BTR-EODLA model (Zelenak et al., 2013), achieved an impressive 98.78% by combining preprocessing, features extraction and parameter optimization.

Table 2. Performance comparison of the reviewed models (Annex).

Reference Number	Method	Accuracy (%)
(Prabha and Singh, 2024)	EfficientNet-B5/B7	99.64
(Ahmed et al., 2024)	Hybrid ViT-GRU	98.97
(Alshuhail et al., 2024)	Sequential CNN	98.00
(Alshuhail et al., 2025)	AlexNet50	98.00
(Zelenak et al., 2013)	BTR-EODLA	98.78

5. Conclusion

A brain tumor is an irregular growth of brain tissue that interferes with the normal functioning of the brain. The primary objective of medical imaging is to develop algorithms capable of extracting accurate and relevant information while minimizing errors. The classification of brain tumors using MRI data is generally divided into four main steps: pre-processing, image segmentation, feature extraction, and tumor classification. However, achieving a fully autonomous system for clinical applications remains challenging due to the variable appearance, irregular size, shape and nature of tumors. This study aims to provide an overview of recent developments in brain tumor research, highlighting imaging techniques, summarising the WHO tumor classification standards and examining the deep learning algorithms applied to brain tumor classification. Compared to region growing methods and traditional machine learning approaches, deep learning techniques offer notable advantages in automated detection and classification of brain tumors, mainly due to their powerful feature learning capabilities. Although the contribution of DL techniques has been significant, the need for a general technique is still an issue.

ANNEX

[1] Arulmani, Dhiyana & Manickam, Rajapriya. (2024). Brain Tumors. Journal of Student Research. 13. 10.47611/jsrhs.v13i2.6694.

[2] H. S. Kim et D. Y. Lee, « Nanomedicine in Clinical Photodynamic Therapy for the Treatment of Brain Tumors », Biomedicines, vol. 10, nº 1, p. 96, janv. 2022, doi: 10.3390/biomedicines10010096.

[3] Solomon Antwi Buabeng, Atta Yaw Agyeman, Samuel Gbli Tetteh, et Lois Azupwah, « Detection of Brain Tumor using Medical Images: A Comparative Study of Machine Learning Algorithms – A Systematic Literature Review », IJLTEMAS, vol. 13, nº 9, p. 77-85, oct. 2024, doi: 10.51583/IJLTEMAS.2024.130907.

[4] I. S. Jacobs and C. P. Bean, “Fine particles, thin films and exchange anisotropy,” in Magnetism, vol. III, G. T. Rado and H. Suhl, Eds. New York: Academic, 1963, pp. 271–350.

[5] K. Elissa, “Title of paper if known,” unpublished.

[6] R. Nicole, “Title of paper with only first word capitalized,” J. Name Stand. Abbrev., in press.

[7] Y. Yorozu, M. Hirano, K. Oka, and Y. Tagawa, “Electron spectroscopy studies on magneto-optical media and plastic substrate interface,” IEEE Transl. J. Magn. Japan, vol. 2, pp. 740–741, August 1987 [Digests 9th Annual Conf. Magnetics Japan, p. 301, 1982].

[8] M. Young, The Technical Writer’s Handbook. Mill Valley, CA: University Science, 1989.

[9] I. Ilic et M. Ilic, « International patterns and trends in the brain cancer incidence and mortality: An observational study based on the global burden of disease », Heliyon, vol. 9, no 7, p. e18222, juill. 2023, doi: 10.1016/j.heliyon.2023.e18222.

[10] Arulmani, D., Manickam, R., & Advisor, #. (n.d.). Brain Tumors. www.JSR.org/hs

[11] C. Prabha et R. Singh, « A Robust Deep Learning Model for Brain Tumor Detection and Classification Using Efficient Net: A Brief Meta-Analysis », J. Adv. Res. Appl. Sci. Eng. Tech., vol. 49, nº 2, p. 26-51, août 2024, doi: 10.37934/araset.49.2.2651.

[12] G. Tiwari, A. Misra, S. Maheshwari, V. Gautam, P. Sharma, and N. K. Trivedi, "Adaptive neuro-fuzzy inference system-fusion-deep belief network for brain tumor detection using MRI images with feature extraction," Biomedical Signal Processing and Control, vol. 103, p. 107387, 2025. DOI: 10.1016/j.bspc.2025.107387.

[13] M. K. Abd-Ellah, A. I. Awad, A. A. M. Khalaf, et A. M. Ibraheem, « Automatic brain-tumor diagnosis using cascaded deep convolutional neural networks with symmetric U-Net and asymmetric residual-blocks », Sci Rep, vol. 14, nº 1, p. 9501, avr. 2024, doi: 10.1038/s41598-024-59566-7.

[14] Md. M. Ahmed et al., « Brain tumor detection and classification in MRI using hybrid ViT and GRU model with explainable AI in Southern Bangladesh », Sci Rep, vol. 14, no 1, p. 22797, oct. 2024, doi: 10.1038/s41598-024-71893-3.

[15] A. Alshuhail et al., « Refining neural network algorithms for accurate brain tumor classification in MRI imagery », BMC Med Imaging, vol. 24, nº 1, p. 118, mai 2024, doi: 10.1186/s12880-024-01285-6.

[16] S. Athisayamani, A. R. Singh, G. P. Joshi, et W. Cho, « Three-Stage Transfer Learning with AlexNet50 for MRI Image Multi-Class Classification with Optimal Learning Rate », CMES, vol. 142, no 1, p. 155-183, 2025, doi: 10.32604/cmes.2024.056129.

[17] S. Anantharajan, S. Gunasekaran, T. Subramanian, and R. Venkatesh, "MRI brain tumor detection using deep learning and machine learning approaches," Measurement: Sensors, vol. 31, p. 101026, 2024. DOI: 10.1016/j.measen.2024.101026.

[18] M. S. Tahosin, M. A. Sheakh, T. Islam, R. J. Lima, and M. Begum, "Optimizing brain tumor classification through feature selection and hyperparameter tuning in machine learning models," Informatics in Medicine Unlocked, vol. 43, p. 101414, 2023. DOI: 10.1016/j.imu.2023.101414.

[19] A. Priya and V. Vasudevan, "Brain tumor classification and detection via hybrid AlexNet-GRU based on deep learning," Biomedical Signal Processing and Control, vol. 89, p. 105716, 2024. DOI: 10.1016/j.bspc.2024.105716.

[20] K. Zelenak, C. Viera, et P. Hubert, « Radiology Imaging Techniques of Brain Tumors », in Clinical Management and Evolving Novel Therapeutic Strategies for Patients with Brain Tumors, T. Lichtor, Éd., InTech, 2013. doi: 10.5772/53470.

REFERENCES

A. Alshuhail et al., « Refining neural network algorithms for accurate brain tumor classification in MRI imagery », BMC Med Imaging, vol. 24, nº 1, p. 118, mai 2024, doi: 10.1186/s12880-024-01285-6.

A. Priya and V. Vasudevan, "Brain tumor classification and detection via hybrid AlexNet-GRU based on deep learning," Biomedical Signal Processing and Control, vol. 89, p. 105716, 2024. DOI: 10.1016/j.bspc.2024.105716.

Arulmani, D., Manickam, R., & Advisor, #. (n.d.). Brain Tumors. www.JSR.org/hs

Arulmani, Dhiyana & Manickam, Rajapriya. (2024). Brain Tumors. Journal of Student Research. 13. 10.47611/jsrhs.v13i2.6694.

C. Prabha et R. Singh, « A Robust Deep Learning Model for Brain Tumor Detection and Classification Using Efficient Net: A Brief Meta-Analysis », J. Adv. Res. Appl. Sci. Eng. Tech., vol. 49, nº 2, p. 26-51, août 2024, doi: 10.37934/araset.49.2.2651.

G. Tiwari, A. Misra, S. Maheshwari, V. Gautam, P. Sharma, and N. K. Trivedi, "Adaptive neuro-fuzzy inference system-fusion-deep belief network for brain tumor detection using MRI images with feature extraction," Biomedical Signal Processing and Control, vol. 103, p. 107387, 2025. DOI: 10.1016/j.bspc.2025.107387.

H. S. Kim et D. Y. Lee, « Nanomedicine in Clinical Photodynamic Therapy for the Treatment of Brain Tumors », Biomedicines, vol. 10, nº 1, p. 96, janv. 2022, doi: 10.3390/biomedicines10010096.

I. Ilic et M. Ilic, « International patterns and trends in the brain cancer incidence and mortality: An observational study based on the global burden of disease », Heliyon, vol. 9, no 7, p. e18222, juill. 2023, doi: 10.1016/j.heliyon.2023.e18222.

I. S. Jacobs and C. P. Bean, "Fine particles, thin films and exchange anisotropy," in Magnetism, vol. III, G. T. Rado and H. Suhl, Eds. New York: Academic, 1963, pp. 271–350.

K. Elissa, "Title of paper if known," unpublished.

K. Zelenak, C. Viera, et P. Hubert, « Radiology Imaging Techniques of Brain Tumors », in Clinical Management and Evolving Novel Therapeutic Strategies for Patients with Brain Tumors, T. Lichtor, Éd., InTech, 2013. doi: 10.5772/53470.

M. K. Abd-Ellah, A. I. Awad, A. A. M. Khalaf, et A. M. Ibraheem, « Automatic brain-tumor diagnosis using cascaded deep convolutional neural networks with symmetric U-Net and asymmetric residual-blocks », Sci Rep, vol. 14, nº 1, p. 9501, avr. 2024, doi: 10.1038/s41598-024-59566-7.

M. S. Tahosin, M. A. Sheakh, T. Islam, R. J. Lima, and M. Begum, "Optimizing brain tumor classification through feature selection and hyperparameter tuning in machine learning models," Informatics in Medicine Unlocked, vol. 43, p. 101414, 2023. DOI: 10.1016/j.imu.2023.101414.

M. Young, The Technical Writer's Handbook. Mill Valley, CA: University Science, 1989.

Md. M. Ahmed et al., « Brain tumor detection and classification in MRI using hybrid ViT and GRU model with explainable AI in Southern Bangladesh », Sci Rep, vol. 14, no 1, p. 22797, oct. 2024, doi: 10.1038/s41598-024-71893-3.

R. Nicole, "Title of paper with only first word capitalized," J. Name Stand. Abbrev., in press.

S. Anantharajan, S. Gunasekaran, T. Subramanian, and R. Venkatesh, "MRI brain tumor detection using deep learning and machine learning approaches," Measurement: Sensors, vol. 31, p. 101026, 2024. DOI: 10.1016/j.measen.2024.101026.

S. Athisayamani, A. R. Singh, G. P. Joshi, et W. Cho, « Three-Stage Transfer Learning with AlexNet50 for MRI Image Multi-Class Classification with Optimal Learning Rate », CMES, vol. 142, no 1, p. 155-183, 2025, doi: 10.32604/cmes.2024.056129.

Solomon Antwi Buabeng, Atta Yaw Agyeman, Samuel Gbli Tetteh, et Lois Azupwah, « Detection of Brain Tumor using Medical Images: A Comparative Study of Machine Learning Algorithms – A Systematic Literature Review », IJLTEMAS, vol. 13, nº 9, p. 77-85, oct. 2024, doi: 10.51583/IJLTEMAS.2024.130907.

Y. Yorozu, M. Hirano, K. Oka, and Y. Tagawa, "Electron spectroscopy studies on magneto-optical media and plastic substrate interface," IEEE Transl. J. Magn. Japan, vol. 2, pp. 740–741, August 1987 [Digests 9th Annual Conf. Magnetics Japan, p. 301, 1982].

author(s) and contributor(s) and not of MJHI and/or the editor(s). MJHI and/or the editor(s) disclaim responsibility for any injury to
people or property resulting from any ideas, methods, instructions or products referred to in the content.

MJHI | Moroccan Journal of Health and Innovation

Article N°2, Vol 1, No 2

Generative AI role in Cardiac MRI Segmentation: A Comprehensive Review

Halima FOUADI [1,2,*], Mohamed KAS [2], Yassine RUICHEK [2], Youssef EL MERABET [1]

1 SETIME Laboratory Faculty of Sciences Ibn Tofail University, Kenitra, Morocco

2 CIAD, UMR 7533, Univ. Bourgogne Franche-Comté, UTBM, Montbéliard, France

* firstname.lastname@utbm.fr

Abstract: The integration of artificial intelligence (AI) has led to notable advancements in medical imaging. However, this progress is limited by the lack of expert-annotated data, particularly for rare pathologies, which hampers scientific research and the training of machine learning models. Generative artificial intelligence meets this need by synthesizing realistic images that correspond to ground-truth data, thereby increasing the data available for training and evaluating Algorithms. In this review, we focus on the cardiac domain, and more specifically on magnetic resonance imaging (MRI), which is an important tool in the diagnosis of cardiac pathologies (the world's leading cause of death). We examine various generative AI methodologies, such as generative adversarial networks (GANs), variational autoencoders (VAEs), and diffusion models, applied to cardiac MRI data. Furthermore, we discuss the implications of these techniques in generating synthetic datasets, augmenting rare pathological cases, and improving segmentation accuracy and diagnostic outcomes. Finally, we highlight the challenges, limitations, and future directions of integrating generative AI into cardiac MRI workflows, aiming to guide further research and clinical translation.

Keywords: Cardiac MRI, Image Segmentation, Generative IA, Synthetic datasets.

Received: April 11, 2025
Revised: May 17, 2025
Accepted: June 10, 2025
Published: July 25, 2025

Citation: FOUADI, F.; KAS, M.; RUICHEK, Y.; EL MERABET, Y. Generative AI role in Cardiac MRI Segmentation: A Comprehensive Review. Moroccan Journal of Health and Innovation (MJHI) 2025, Vol 1, No 2. https://mjhi-smb.com

1. Introduction

Cardiac magnetic resonance imaging is an important modality in the diagnosis, intervention and management of cardiovascular diseases which is one of the most common causes of death in the world according to the world health organization (Jafari et al., 2023) . By providing high-resolution images of the heart, accurate identification of anatomy, functions and tissues characterization, it can identify cardiac pathologies such as myocardial infarction, ischemic heart disease, cardiomyopathy, and congenital heart defects. The application of cardiac MRI is based on the segmentation of heart structures and regions of interest for analysis. However, manual segmentation is time-consuming and labor-intensive, making it susceptible to inter-observer variability. This highlights the strong need for automated segmentation methods (Kanakatte et al., 2022).

The integration of artificial intelligence (AI) into the automation of cardiac segmentation has experienced significant advancements in recent years. In particular, the adoption of deep learning techniques such as recurrent neural networks (RNNs) and convolutional neural networks (CNNs), has revolutionized the field by achieving exceptional accuracy and efficiency. These methods excelled over traditional algorithms in effectively delineating complex anatomical structures and variations in cardiac magnetic resonance imaging (MRI) data (Taraboulsi et al., 2023). Nevertheless, these models face significant challenges mainly in terms of relying on a database with expert-annotation. Considering these limitations, generative artificial intelligence can meet the need by generating realistic synthetic data, thus increasing the diversity and quantity of available databases, while preserving pathology-related characteristics. By leveraging techniques such as (GANs), (VAEs), and diffusion models, generative AI can synthesize realistic cardiac MRI images with corresponding ground-truth annotations. These synthetic datasets have the potential to augment existing ones and enhance the training of segmentation algorithms. and improving diagnostic accuracy by enabling more robust and diverse model development (Al Khalil et al., 2023).

In this review, we aim to provide a comprehensive analysis of the role of generative AI in cardiac MRI segmentation. We begin by outlining the different techniques of generative AI followed by an exploration of state-of-the-art databases devoted to cardiac MRI semantic segmentation. Next, we discuss the existing works in the literature and their contributions to synthetic data. Finally, we examine the challenges and limitations of these approaches and propose future directions to guide the integration of generative AI into cardiac MRI workflows.

2. BACKGROUND

Generative AI is an Artificial intelligence field that can generate realistic images, text and sounds by using deep learning algorithms that are trained on large amounts of data. Generative AI has seen tremendous growth in recent years and has been applied to a wide range of practical and creative fields, from art and entertainment to healthcare and engineering. We briefly introduce the different generative AI paradigms in the following.

- Generative Adversarial Networks:

Presented by Goodfellow et al. in 2014 (Goodfellow et al., 2014) ,are a novel class of deep learning techniques (a type of artificial intelligence algorithm). GANs consist of two models: a discriminator D, which is tasked with distinguishing between real and fake images, and a generator G, which learns to create realistic data through training. One type of GANs that is widely used in medical imaging is Pix2Pix GAN that is designed for image-to-image translation tasks. Pixel-to-pixel, indicating that the model operates on a pixel-level mapping between input and output images. The goal is to learn a mapping between an input and a corresponding output image. Pix2pix uses a conditional GAN architecture, where both discriminator and generator are conditioned on the input image. This adversarial training process allows the model to learn to generate high-quality image transformations (Isola et al., 2024).

- Diffusion models:

Diffusion model is a class of deep learning models used for generating high-quality images from text descriptions. The name comes from the idea of "diffusion" as a process of gradually transforming noise into a desired output, and "stable" reflects the model's ability to produce consistent high-quality results(Rombach et al., 2022). Thanks to this iterative denoising process, Stable Diffusion models reach higher quality than GANs. However, their application in medical imaging remains limited due to the scarcity of training data with text annotations and their high computational complexity.

- VAE:

Is a deep learning model designed to generate data similar to the ground truth by leveraging the principles of autoencoders. It consists of three main components: an encoder, a decoder, and a loss function. The goal of VAE is to learn both an encoder and a decoder that map data x to and from a continuous latent space z. The encoder receives an input image and reduces it to a more compact vector in latent space, capturing the essential features of the data. The decoder then processes this

compressed vector to reconstruct it, transforming it back into a format that facilitates prediction of the output image. This process ensures that the data produced is very similar to the original data, while preserving the diversity of the results (Kusner et al., 2025), (Kingma and Welling, 2013).

3. DATASET

Annotated datasets play a crucial role in the training and evaluation of GAI models. In the context of CMRI datasets, it enables models to learn complex patterns and generate realistic, high-quality results. This section (Table 1) presents some of the most popular datasets available from CMRI.

Table 1 : Summary of available datasets of CMRI for semantic segmentation (Annex).

Reference	Dataset	Number of cases	Citations	Years
(Bernard et al., 2018)	ACDC	100 train 50 test	1848	2018
(Campello et al., 2021)	M&Ms	175 train 136 test		2020
(Perry et al., 2009)	SCD	45 Cine	445	2009
(Kadish et al., 2009)	LVSC	100 train 100 test	134	2011
(Petitjean et al., 2015)	RVSC	16 train 32 test	264	2015
(Andreopoulos et al., 2007)	York University	33 Cine	393	2008

4. APPLICATIONS OF GENERATIVE AI IN CARDIAC MR IMAGING

The state of the art in GAI applications for cardiac MR imaging can be classified into two main approaches: studies that focus exclusively on synthetic scan generation without pixel-wise semantic labels, and those that integrate image generation with segmentation. The following items briefly present the papers corresponding to each of these two approaches, highlighting the main contributions.

- **Unlabeled MRI Scan generation**

(Yoon et al., 2023): The Sequence-Aware Diffusion Model (SADM) was introduced for the generation of longitudinal medical images, such as cardiac and brain MRIs. This model learns to generate medical images from image sequences, considering their temporal order. In this way, it can synthesize the last image of a cardiac cycle from the first image of that cycle. The model was

evaluated on public cardiac MRI data, using the ACDC database.

(Kim and Ye, 2022): This study proposed a model for generating 4D cardiac cycle images, enabling the visualization of continuous anatomical changes. This model is particularly suited for generating 4D images of the cardiac cycle, allowing for continuous and progressive visualization of anatomical deformations throughout the cardiac cycle. This model relies on a structure similar to 3D UNet, with skip connections to preserve essential spatial information. This architecture helps generate high-quality volumetric images. It includes a Deformation Module based on VoxelMorph-1that generates deformation fields in 3D images. This module enables smooth deformation between the different phases of the cardiac cycle. Scan to scan without segmentation.

(Campello et al., 2022): This study presented a Conditional GAN (cGAN) for synthesizing heart scans of different ages using only cross-sectional data. The used cGAN architecture is based on a U-Net architecture with residual blocks and attention mechanisms. The model is conditioned by age and body mass index (BMI) to adjust images according to these covariates. A Wasserstein-GAN algorithm with gradient penalty (WGAN-GP) is used to stabilize training.

- **Labled**

(Ossenberg-Engels and Grau, 2020) : The authors proposed a Conditional Generative Adversarial Network to predict cardiac deformation between end-diastolic (ED) and end-systolic (ES) frames. Using the UK Biobank dataset, their model learned a deterministic mapping between ED and ES short-axis frames, enabling the modeling of cardiac sequences and the functional behavior of the heart. This learning helped to increase the data by transforming the scans from each phase to the other one respecting their corresponding semantic labels.

(Al Khalil et al., 2022): This framework, trained on the M&Ms dataset, focuses on right ventricle segmentation and integrates three key components: Detection of the region of interest (ROI) by cropping the image to center the heart within the field of view (FOV), image synthesis through the application of a mask-conditional GAN that learns the mapping from segmentation labels to corresponding realistic images. The application of random elastic deformation, morphological dilation, and erosion to the labels to generate anatomical variations of the heart, including pathological cases. Finally, a modified U-Net network was proposed to enhance cardiac segmentation through the integration of both real and synthetic images.

(Al Khalil et al., 2023): The authors proposed a conditional synthesis approach using GANs to generate realistic cardiac MRI images in the short-axis view. This study is based on three main steps: image synthesis, a conditional synthesis approach based on GANs is used to generate realistic cardiac MRI images in short-axis view. The quality of these images is enhanced using labels of different tissues surrounding the heart, generated by a multi-tissue segmentation network trained on simulated XCAT-based images. This strategy helped the GAN to generate coherent MRI scans of the heart and its surroundings. The next steps of their framework consist of region of interest (ROI) detection and heart chamber segmentation using the generated images to train a convolutional neural network (CNN), based on a U-Net architecture, for heart chamber segmentation (right ventricle, left ventricle and myocardium).

(Diller et al., 2020): This study utilized cardiac MRIs from patients with Tetralogy of Fallot to develop and compare segmentation models. Progressive GANs (PG- GANs) are trained, on the collected data sourced from 14 German centers, to generate synthetic MRI frames. The synthetized frames were manually segmented to create training data for a U-Net based segmentation model. To evaluate the quality of synthetic data a random selection of 200 PG-GAN-generated images and 200 original MRI images was submitted to human investigators who had to identify the PG-GAN-generated image which reflected their realism.

(Amirrajab et al., 2022): This study introduced a two-module framework for generating high-fidelity cardiac MR images. The first module utilizes a U-Net model for multi-tissue segmentation of cardiac MR images. The output of this module is a segmentation mask that labels various tissues, including the myocardium (MYO), right ventricle (RV), and left ventricle (LV). These segmentation masks serve as input labels for generating new images using a cGAN trained on M&Ms dataset, which produces realistic cardiac MR images based on the anatomical structures encoded in the segmentation masks. The simulated anatomies of virtual subjects are derived from the 4D XCAT phantoms, and the images are simulated through a physics-based simulation tool that implements the Bloch equations for cine studies.

(Kim and Ye, 2022): DiffuseMorph is an unsupervised model for deformable image registration using diffusion models. Image registration aims to align multiple images taken from different angles or at different time points by deforming them to match a reference image or atlas. DiffuseMorph achieves deformable image registration in an unsupervised manner by utilizing a diffusion model. The training is based on ACDC benchmarks. These data were resampled, normalized, and cropped to fit the model.

(Amirrajab et al., 2020): This study proposed a method with two different configurations one using only the ground truth annotations available for the heart and another increasing the number of labels into 8 classes encompassing the organs surrounding the heart when training the XCAT-GAN model. Their pipeline is composed of three cascaded models: (1) a modified version of UNet that predicts multi-tissue segmentation maps from real images, used only in 8-class image synthesis. (2) a conditional GAN architecture trained on pairs of real images and label maps (4 or 8 classes) to generate synthetic images based on XCAT labels. (3) an adapted version of U-Net in 2D, used to evaluate new synthetic images and their corresponding labels in various experimental scenarios including only valid ones in the augmented training dataset.

(Abbasi-Sureshjani et al., 2020): The authors proposed a GAN-based approach for synthesizing 4D (3D+t) cardiac MR images, using the 4D XCAT model as ground truth. To preserve the spatial and semantic information of the reference anatomy, they used the SPADE (Semantic Image Synthesis with Spatially Adaptive Normalization) model originally proposed for semantic controlled generation. For training, they used images from the ACDC database with their corresponding segmentation masks. During inference, they replace the segmentation masks with voxelated 4D labels from the XCAT to generate new 4D MRI images.

(Lustermans et al., 2022): This work aimed to improve cardiac MRI scan segmentation with late contrast (LGE), particularly in contexts with limited data sets. The first approach involves dividing the segmentation task into simpler sub-problems, and the second relies on the use of synthetic data to increase the amount of data available. A cascade pipeline method has been proposed, comprising three deep-based blocks. The first identifies the left ventricle, the second delineates the left ventricular myocardium, and the third segments the regions of myocardial infarction. The segmentation-conditioned synthetic data generator (using a GAN) was used to augment the training data. The study also showed that augmentation by synthetic data improves scar segmentation, particularly in challenging datasets with noise and artifacts.

(Skandarani et al., 2020): This paper proposed a model to produce highly realistic MRI images (100k) with pixel-accurate ground truth for cardiac segmentation in cine-MR combining Variational Autoencoder (VAE) with SPADE-GAN. VAE network is trained to learn the latent representations of cardiac shapes, enabling the model to capture the variations in heart shapes across individuals. On the other hand, SPADE-GAN generates realistic MR images based on an anatomical map input. The GAN learns to generate images whose cardiac structures align with the shapes generated by the VAE.

Figure 1 illustrates a mapping of the reviewed literature works based on their ability to generate

labelled scans and also depending on the required inputs (Scan, Scan+Label, Label).

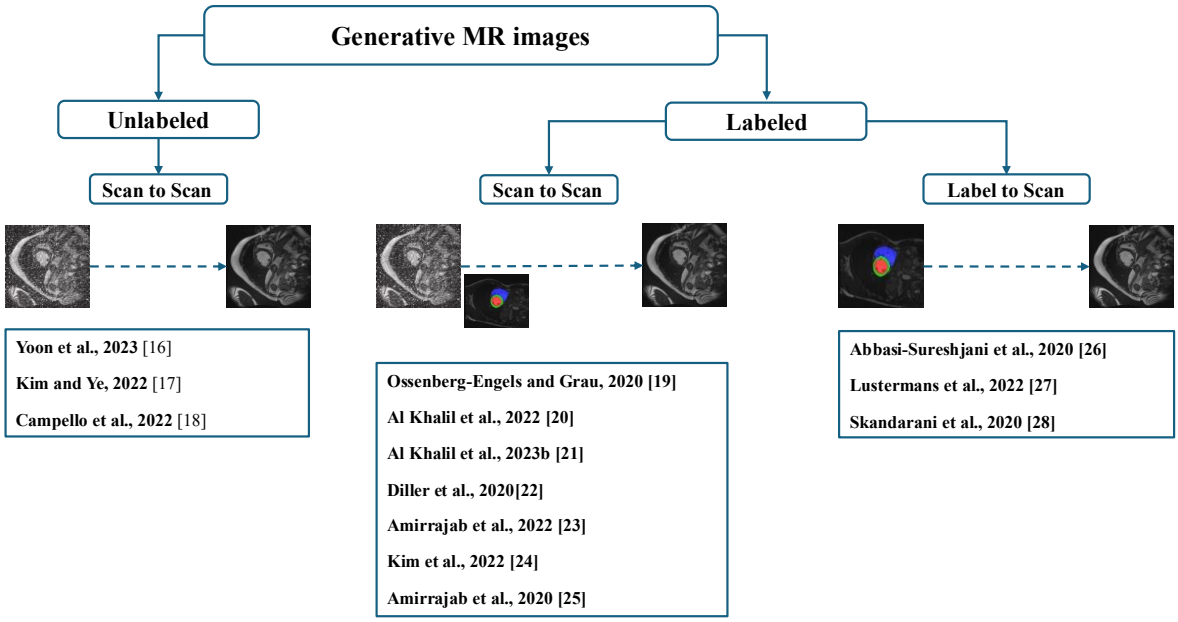

Taxonomy of existing works in cardiac MRI segmentation.

5.OPENING

Generative AI has enabled significant advances in the improvement of medical image databases, particularly for rare or difficult-to-annotate cases, such as cardiac MRI. However, beyond the generation of realistic and diverse images to train segmentation models, many other applications are possible in this field, notably decision-making through image classification, as well as temporal image synthesis to study the evolution of cardiac pathologies over time, an important area in the monitoring of patients with chronic cardiovascular diseases.

6.Conclusion:

The integration of generative AI into cardiac imaging, particularly for MRI segmentation, represents an essential lever for cardiovascular management. Techniques such as GANs, VAEs and diffusion models have demonstrated their potential to generate realistic images and increase the diversity of training data, while improving the accuracy of segmentation models. However, several challenges remain, particularly regarding the quality of the images generated, their generalizability to varied clinical populations and the need for high-quality annotated data. As technology continues to advance, these models could not only enrich available databases but also improve diagnostic and clinical outcomes. The future of GAI in cardiac MRI lies in better clinical integration, with particular attention

to model validation and adaptation to specific patient needs.

Acknowledgements

The authors declare that they have no known competing financial interests or personal relationships that could have appeared to influence the work reported in this paper.

References :

A. Andreopoulos and J. K. Tsotsos, “Efficient and generalizable statistical models of shape and appearance for analysis of cardiac MRI,” Med Image Anal, vol. 12, no. 3, pp. 335–357, Jun. 2008, doi: 10.1016/j.media.2007.12.003.

A. H. Kadish et al., “Rationale and Design for the Defibrillators To Reduce Risk By Magnetic Resonance Imaging Evaluation (DETERMINE) Trial,” J Cardiovasc Electrophysiol, vol. 20, no. 9, pp. 982–987, Sep. 2009, doi: 10.1111/j.1540-8167.2009.01503.x.

A. Kanakatte, D. Bhatia, and A. Ghose, “3D Cardiac Substructures Segmentation from CMRI using Generative Adversarial Network (GAN),” in 2022 44th Annual International Conference of the IEEE Engineering in Medicine & Biology Society (EMBC), Jul. 2022, pp. 1698–1701. doi: 10.1109/EMBC48229.2022.9871950.

B. Kim and J. C. Ye, “Diffusion Deformable Model for 4D Temporal Medical Image Generation,” in Medical Image Computing and Computer Assisted Intervention – MICCAI 2022, L. Wang, Q. Dou, P. T. Fletcher, S. Speidel, and S. Li, Eds., Cham: Springer Nature Switzerland, 2022, pp. 539–548. doi: 10.1007/978-3-031-16431-6_51.

B. Kim, I. Han, and J. C. Ye, “DiffuseMorph: Unsupervised Deformable Image Registration Using Diffusion Model,” Sep. 29, 2022, arXiv: arXiv:2112.05149. doi: 10.48550/arXiv.2112.05149.

C. Petitjean et al., “Right ventricle segmentation from cardiac MRI: A collation study,” Medical Image Analysis, vol. 19, no. 1, pp. 187–202, Jan. 2015, doi: 10.1016/j.media.2014.10.004.

D. R. P. R. M. Lustermans, S. Amirrajab, M. Veta, M. Breeuwer, and C. M. Scannell, “Optimized automated cardiac MR scar quantification with GAN-based data augmentation,” Computer Methods and Programs in Biomedicine, vol. 226, p. 107116, Nov. 2022, doi: 10.1016/j.cmpb.2022.107116.

G.-P. Diller et al., “Utility of deep learning networks for the generation of artificial cardiac magnetic resonance images in congenital heart disease,” BMC Med Imaging, vol. 20, p. 113, Oct. 2020, doi: 10.1186/s12880-020-00511-1.

I. Goodfellow et al., “Generative Adversarial Nets,” in Advances in Neural Information Processing Systems, Curran Associates, Inc., 2014. Accessed: Dec. 23, 2024. [Online]. Available: https://proceedings.neurips.cc/paper_files/paper/2014/hash/5ca3e9b122f61f8f06494c97b1afccf3-Abstract.html

J. El-Taraboulsi, C. P. Cabrera, C. Roney, and N. Aung, “Deep neural network architectures for cardiac image segmentation,” Artificial Intelligence in the Life Sciences, vol. 4, p. 100083, Dec. 2023, doi: 10.1016/j.ailsci.2023.100083.

J. Ossenberg-Engels and V. Grau, "Conditional Generative Adversarial Networks for the Prediction of Cardiac Contraction from Individual Frames," in Statistical Atlases and Computational Models of the Heart. Multi-Sequence CMR Segmentation, CRT-EPiggy and LV Full Quantification Challenges, M. Pop, M. Sermesant, O. Camara, X. Zhuang, S. Li, A. Young, T. Mansi, and A. Suinesiaputra, Eds., Cham: Springer International Publishing, 2020, pp. 109–118. doi: 10.1007/978-3-030-39074-7_12.

J. S. Yoon, C. Zhang, H.-I. Suk, J. Guo, and X. Li, "SADM: Sequence-Aware Diffusion Model for Longitudinal Medical Image Generation," vol. 13939, 2023, pp. 388–400. doi: 10.1007/978-3-031-34048-2_30.

Kingma, D. P., & Welling, M. (2013). Auto-encoding variational bayes. arXiv preprint arXiv:1312.6114.

M. J. Kusner, B. Paige, and J. M. Hernández-Lobato, "Grammar Variational Autoencoder," in Proceedings of the 34th International Conference on Machine Learning, PMLR, Jul. 2017, pp. 1945–1954. Accessed: Jan. 02, 2025. [Online]. Available: https://proceedings.mlr.press/v70/kusner17a.html

M. Jafari et al., "Automated diagnosis of cardiovascular diseases from cardiac magnetic resonance imaging using deep learning models: A review," Computers in Biology and Medicine, vol. 160, p. 106998, Jun. 2023, doi: 10.1016/j.compbiomed.2023.106998.

O. Bernard et al., "Deep Learning Techniques for Automatic MRI Cardiac Multi-Structures Segmentation and Diagnosis: Is the Problem Solved?," IEEE Transactions on Medical Imaging, vol. 37, no. 11, pp. 2514–2525, Nov. 2018, doi: 10.1109/TMI.2018.2837502.

P. Isola, J.-Y. Zhu, T. Zhou, and A. A. Efros, "Image-To-Image Translation With Conditional Adversarial Networks," presented at the Proceedings of the IEEE Conference on Computer Vision and Pattern Recognition, 2017, pp. 1125–1134. Accessed: Dec. 24, 2024. [Online]. Available: https://openaccess.thecvf.com/content_cvpr_2017/html/Isola_Image-To-Image_Translation_With_CVPR_2017_paper.html

R. Perry, L. Yingli, C. Kim, P. Gideon, A. J. Dick, and G. A. Wright, "Evaluation Framework for Algorithms Segmenting Short Axis Cardiac MRI.," The MIDAS Journal, Jul. 2009, doi: 10.54294/g80ruo.

R. Rombach, A. Blattmann, D. Lorenz, P. Esser, and B. Ommer, "High-Resolution Image Synthesis With Latent Diffusion Models," presented at the Proceedings of the IEEE/CVF Conference on Computer Vision and Pattern Recognition, 2022, pp. 10684–10695. Accessed: Dec. 24, 2024. [Online]. Available: https://openaccess.thecvf.com/content/CVPR2022/html/Rombach_High-Resolution_Image_Synthesis_With_Latent_Diffusion_Models_CVPR_2022_paper.html

S. Abbasi-Sureshjani, S. Amirrajab, C. Lorenz, J. Weese, J. Pluim, and M. Breeuwer, "4D Semantic Cardiac Magnetic Resonance Image Synthesis on XCAT Anatomical Model," May 20, 2020, arXiv: arXiv:2002.07089. doi: 10.48550/arXiv.2002.07089.

S. Amirrajab et al., "XCAT-GAN for Synthesizing 3D Consistent Labeled Cardiac MR Images on Anatomically Variable XCAT Phantoms," Jul. 31, 2020, arXiv: arXiv:2007.13408. doi: 10.48550/arXiv.2007.13408.

S. Amirrajab, Y. Al Khalil, C. Lorenz, J. Weese, J. Pluim, and M. Breeuwer, "Label-informed cardiac magnetic resonance image synthesis through conditional generative adversarial networks," Computerized Medical Imaging and Graphics, vol. 101, p. 102123, Oct. 2022, doi: 10.1016/j.compmedimag.2022.102123.

V. M. Campello et al., "Cardiac aging synthesis from cross-sectional data with conditional generative adversarial networks," Front. Cardiovasc. Med., vol. 9, Sep. 2022, doi: 10.3389/fcvm.2022.983091.

V. M. Campello et al., "Multi-Centre, Multi-Vendor and Multi-Disease Cardiac Segmentation: The M&Ms Challenge," IEEE Transactions on Medical Imaging, vol. 40, no. 12, pp. 3543–3554, Dec. 2021, doi: 10.1109/TMI.2021.3090082.

Y. Al Khalil, S. Amirrajab, C. Lorenz, J. Weese, J. Pluim, and M. Breeuwer, "On the usability of synthetic data for improving the robustness of deep learning-based segmentation of cardiac magnetic resonance images," Medical Image Analysis, vol. 84, p. 102688, Feb. 2023, doi: 10.1016/j.media.2022.102688.

Y. Al Khalil, S. Amirrajab, C. Lorenz, J. Weese, J. Pluim, and M. Breeuwer, "On the usability of synthetic data for improving the robustness of deep learning-based segmentation of cardiac magnetic resonance images," Medical Image Analysis, vol. 84, p. 102688, Feb. 2023, doi: 10.1016/j.media.2022.102688.

Y. Al Khalil, S. Amirrajab, J. Pluim, and M. Breeuwer, "Late Fusion U-Net with GAN-Based Augmentation for Generalizable Cardiac MRI Segmentation," in Statistical Atlases and Computational Models of the Heart. Multi-Disease, Multi-View, and Multi-Center Right Ventricular Segmentation in Cardiac MRI Challenge, vol. 13131, E. Puyol Antón, M. Pop, C. Martín-Isla, M. Sermesant, A. Suinesiaputra, O. Camara, K. Lekadir, and A. Young, Eds., in Lecture Notes in Computer Science, vol. 13131. , Cham: Springer International Publishing, 2022, pp. 360–373. doi: 10.1007/978-3-030-93722-5_39.

Y. Skandarani, N. Painchaud, P.-M. Jodoin, and A. Lalande, "On the effectiveness of GAN generated cardiac MRIs for segmentation," May 22, 2020, arXiv: arXiv:2005.09026. doi: 10.48550/arXiv.2005.09026.

MJHI | Moroccan Journal of Health and Innovation

Article N°3, Vol 1, No 2

Three-dimensional model of the human ear using finite element method to study the effects of bone and cartilage on umbo displacement

Lucrece Barbara Penpen Komgue [1,2,*], Safaa Assif [2], Adil Faiz [1], Joël Ducourneau [1], and Abdelowahed Hajjaji [2]

1 Laboratory of Energetics and Theoretical and Applied Mechanics, Lorraine University, Nancy, France

2 Laboratory of Engineering Sciences for Energy, National School of Applied Sciences, El Jadida, Morocco

* penpenkomguelucrece@gmail.com

Abstract: The three-dimensional modeling of the human ear has emerged as a relevant alternative to experiments conducted on cadavers, owing to its accessibility while providing comparable benefits for students (Jenks et al., 2021). Two primary methods for generating 3D computer models of the human ear are documented in the literature: the µCT imaging method and the finite element method, which is based on a numerical approach.

The µCT (Micro-computed tomography) imaging approach involves performing high-resolution scans at a microscopic scale of the human ear using X-rays, with the aim of reconstructing it in two or three dimensions. In contrast, the finite element method employs documented dimensions and geometric shapes from existing literature to model the human ear using work plans.

The present study will concentrate on the finite element method. It is imperative to acknowledge that most of the three-dimensional models of the human ear cited in the extant literature do not account for bony and cartilaginous structures (Gan et al., 2004), (Zhang and Gan, 2013), (Liu et al., 2022).

This research aims to develop a comprehensive three-dimensional model of the human external ear, which includes the auditory canal, skin, bone, cartilage, and tympanic membrane. This model is intended to facilitate an examination of how bone and cartilage influence the displacement of the umbo. In this constructed model, both the ossicular chain and cochlea were substituted with a mechanical impedance represented by a mass-spring-damper system.

The findings from this study suggest that both bone and cartilage contribute to the displacement of the umbo within a frequency range of 2500 to 6300 Hz.

Keywords: Three-dimensional modeling, Finite Element Methods, human ear, displacement of the umbo.

Received: April 08, 2025
Revised: May 21, 2025
Accepted: June 06, 2025
Published: July 25, 2025

Citation: Senhaji A. Interoperability of Health Systems: Challenges and Perspectives for Improving Care. Moroccan Journal of Health and Innovation (MJHI) 2025, Vol 1, No 2. https://mjhi-smb.com

1. Introduction

The human ear serves as the organ responsible for auditory perception. Its primary function encompasses the amplification, transmission, and conversion of acoustic waves from the environment into electrical impulses that are subsequently interpreted by the brain through the auditory nerve. The structure of the ear can be categorized into three distinct sections: the outer ear, which includes the pinna and external auditory canal; the middle ear, consisting of the tympanic membrane and ossicular chain (comprising malleus, incus, and stapes); and the inner ear, which incorporates both the vestibular system and cochlea.

In the literature, two principal approaches are described for three-dimensional geometric modeling of the human ear: one based on imaging scans and another grounded in finite element methods.

The imaging scan approach entails capturing high-resolution scans of the human ear at a microscopic scale using X-rays to reconstruct its geometric shape in two or three dimensions. Conversely, the finite element method relies on solving differential equations and utilizes documented dimensions and geometric descriptions of the human ear found in literature to model its geometric form.

Regardless of the modeling approach employed, the three-dimensional (3D) modeling of the human ear has emerged as a significant alternative to experiments conducted on cadavers, owing to its accessibility while providing comparable benefits for students. In addition to its educational contributions, 3D modeling of the human ear facilitates various studies regarding the functioning of the auditory system, as well as examining the impact of auditory prosthetics on this system.

In the present study, we will concentrate on employing the finite element method for modeling purposes. Existing literature reveals that the majority of three-dimensional models of the human ear created using this methodology do not incorporate bony and cartilaginous tissues (Gan et al., 2004), (Zhang and Gan, 2013), (Liu et al., 2022).

2. Finite element model

Our approach to creating the 3D human ear model involved the following. The auditory canal was modeled using cross-sections with variable diameters and orientations (Figure 1.a). By applying the loft operation to all the cross-sections defining the auditory canal, a 3D geometry of an "***S***" shaped canal was generated (Figure 1.b). Both parts of the tympanic membrane were modeled. Its geometry is conical (Daphalapurkar et al., 2009), with a surface area of 123.5 mm², a uniform thickness of 0.1 mm, a height of 1.7 mm (Lee et al., 2006), (Wever and Lawrence, 1954) (Figure 2.a), and it forms an

inclination angle of 50 degrees with the auditory canal (Stinson and Lawton, 1989) (Figure 2.b). The skin was modeled with a decreasing thickness ranging from 1 mm to 0.8 mm at the cartilaginous part and from 0.8 mm to 0.5 mm at the bony part (Ballachanda, 2013), (Perry and Shelley, 1955), (Brummund et al., 2014) (Figure 3.a). The cartilage was modeled over a length of 15 mm from the entrance of the canal, exhibiting a decreasing thickness from 13.6 mm to 8 mm relative to the auditory canal (Figure 3.b). The bone was modeled over the other half of the auditory canal, showing a varying thickness from 6.9 mm to 8.8 mm relative to the auditory canal (Figure 3.c).

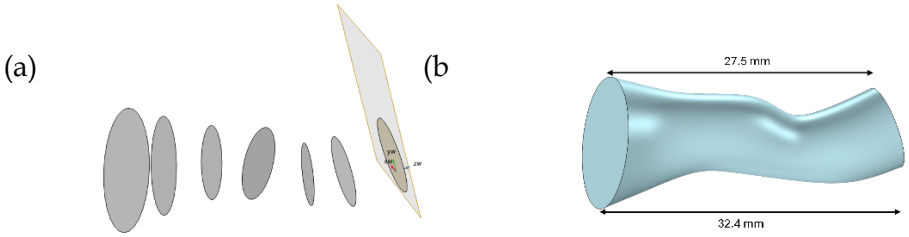

Figure 1. Geometric model and dimensions of the auditory canal.

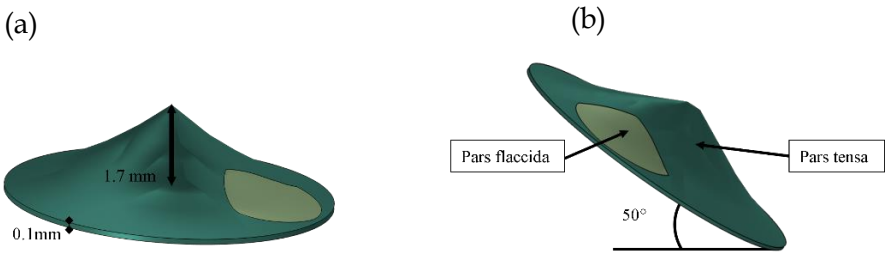

Figure 2. Geometric model and dimensionsof the eardrum.

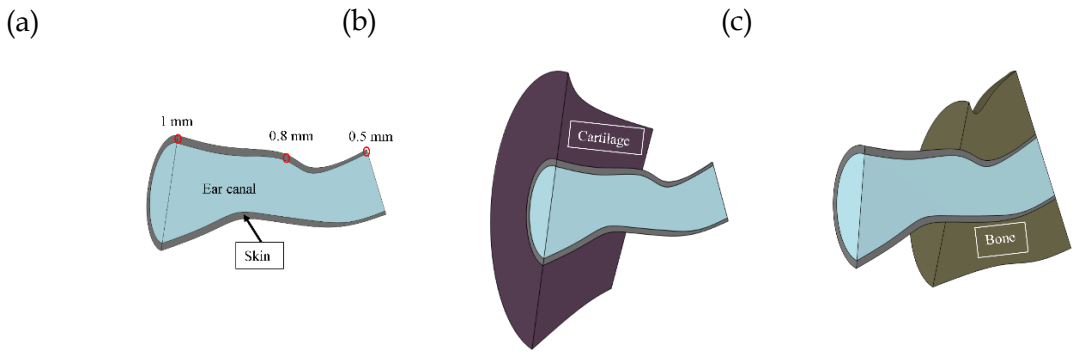

Figure 3. Geometric model and dimensions of (a) the skin, (b) cartilage and (c) bone.

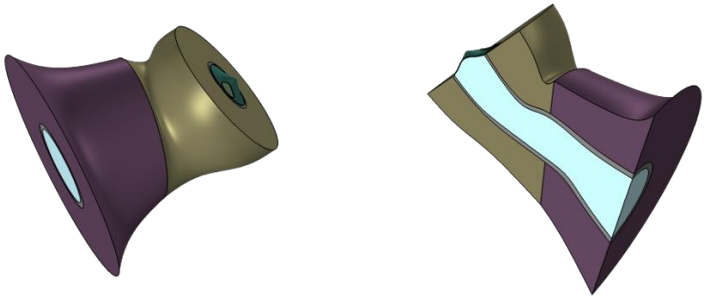

Figure 4. 3D model of the human ear.

3. Boundary conditions

For this study, the auditory canal was defined as a fluid domain filled with air. The skin, bone, cartilage, and tympanic membrane were delineated as solid domains.

To restrict any movement in space, the tympanic ring, the circumferential boundaries of the skin, bone, and cartilage were fixed using a fixed constraint displacement ($u_x=u_y=u_z=0$).

The loading of the ear components located directly after the tympanic membrane (the malleus, incus, stapes and cochlea) has been replaced by an equivalent mechanical impedance represented by a mass-spring-damper system. For this mechanical impedance, the value of the spring constant ‘K’ and the friction coefficient ‘d’ used are respectively 120 N/m and 0.2 N·s/m.

A plane wave of 0.2 Pa corresponding to 80 dB was applied at the entrance of the auditory canal. The interfaces between the solid domains and the auditory canal were expressed through acoustic-structural

coupling.

Material properties

The materials' properties have been taken from the literature and are presented in Table 1.

Table 1: Material properties of the proposed model

		Young's modulus (MPa)	Density (kg/m^3)	Poisson's ratio	Loss factor
Bone	Value	11316	1714	0.3	0.01
	Reference	(Shaw and Stinson, 1981)	(Shaw and Stinson, 1981)	(Delille et al., 2007)	n/a
Cartilage	Value	7.2	1080	0.26	0.05
	Reference	(Peterson and Dechow, 2003)	(Grellmann et al., 2006)	(Peterson and Dechow, 2003)	n/a
Skin	Value	0.5	1100	0.4	0.1
	Reference	(Cox and Peacock, 1979)	(Sarvazyan et al., 1995)	n/a	n/a
Tympanic membrane	Value	33.3	1200	0.3	–
	Reference	(Cameron, 1991)	(Cameron, 1991)	n/a	–

The auditory canal is defined as an air-filled domain with a density of ρ_{air} = 1.20 kg/m³ and a speed of sound of c_{air} = 343.2 m/s.

4. Results and interpretations

In this section, we will examine the impact of bone and cartilage on the displacement of the umbo.

Here, we examine two configurations. The first is that of a 3D model of the human ear, as described in section 2. For reference, this foundational model comprises the auditory canal, cartilage, skin, bone, and tympanic membrane. To investigate the influence of bone and cartilage on umbo displacement within the proposed model, we removed the skin, bone, and cartilage from the proposed model. Subsequently, we substituted the skin with a physiological impedance.

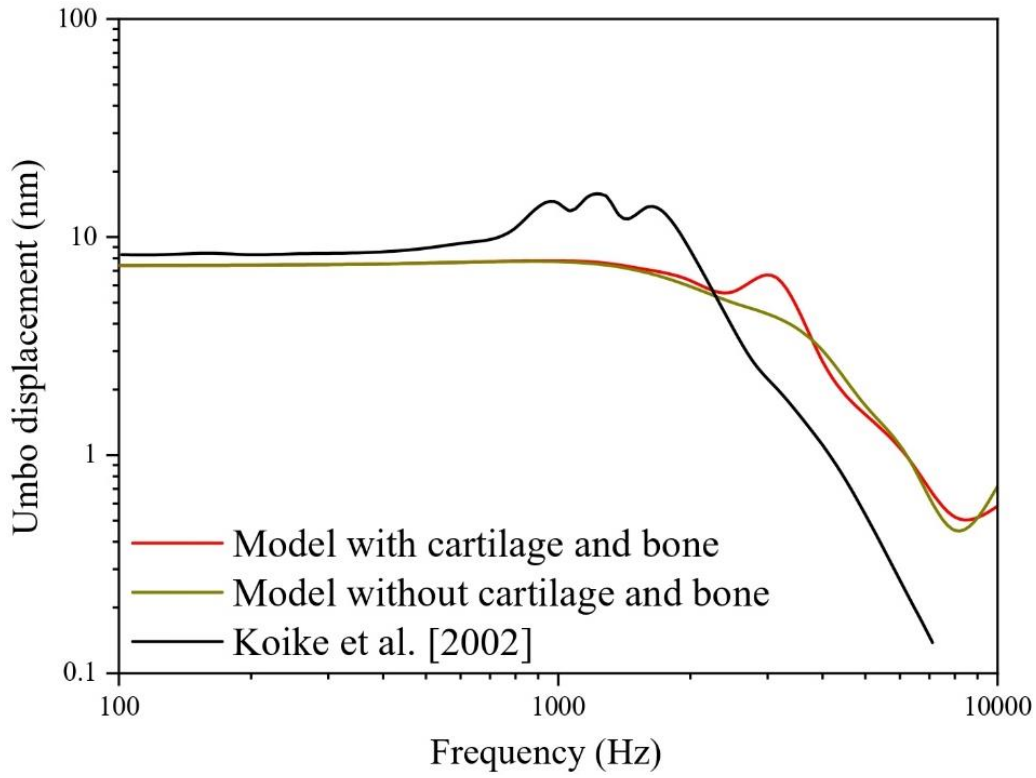

Figure 5. Umbo displacement at 80 dB SPL.

This figure presents the comparative results of the displacement of the umbo induced by an acoustic pressure of 80 dB at the entrance of the ear canal. In this figure, we have the results of the 3D model of the human ear developed with or without bony and cartilaginous tissues, and the results of Koike et al. (Koike et al., 2002).

First, we have a comparison between the results of the 3D model of the human ear developed when the cartilaginous and bony tissues are taken into account or not. The comparison of these two results highlights the effect of bone and cartilage on the displacement of the umbo. Indeed, we find that bony and cartilaginous tissues have a frequency range of interest between 2500 and 6300 Hz.

Secondly, we have a comparison between the results of our model and those of Koike et al. (Koike et al., 2002). This comparative study allows us first to validate the modeling approach, the geometric dimensions, and the parameters used. Then, we observe that the results of the model taking into account the bone and cartilage present a nearly similar trend to those of Koike et al. (Koike et al., 2002). Although we have a shift in the peak of the maximum displacement of the umbo. Indeed, Koike et al. obtained the maximum displacement around 1250 Hz, but with the 3D model of the human ear with the bone and cartilage, the peak of the maximum displacement is observed around 2500 Hz. One of the reasons that could explain this shift might be the fact that Koike et al. (Koike et

al., 2002) modeled the ossicular chain, the ligaments, and tendons of the middle ear and replaced the cochlea with a mechanical impedance, whereas in our model, the ossicular chain and the cochlea were represented by the impedance of a mass-spring-damper system.

5. Conclusion

This study aimed to develop a 3D human ear model to investigate how bony and cartilaginous tissues influence umbo displacement. The model includes the auditory canal, bone, skin, cartilage, and tympanic membrane (pars tensa and pars flaccida). The middle ear's influence was accounted for by replacing the ossicular chain and cochlea with an equivalent mass-spring-damper impedance.

Our findings indicate that bone and cartilage influence the response between 2500 and 6300 Hz. A comparison with Koike et al. (Koike et al., 2002) revealed discrepancies at various frequencies, which we attribute to differences in modeling methodology. Specifically, our model simplifies the ossicular chain and cochlea into a mass-spring-damper impedance, whereas Koike et al. explicitly modeled the ossicular chain, tendons, and ligaments while representing the cochlea with an impedance. To enhance our model, future work will incorporate detailed modeling of the ossicular chain, ligaments, tendons, and cochlea

References

A. P. Sarvazyan et al., "Biophysical Bases of Elasticity Imaging," 1995, pp. 223–240. doi: 10.1007/978-1-4615-1943-0_23.

Bopanna B. Ballachanda, The human ear canal, Second edition. Plural Publishing, 2013.

C. M. Jenks, V. Patel, B. Bennett, B. Dunham, and C. M. Devine, "Development of a 3-Dimensional Middle Ear Model to Teach Anatomy and Endoscopic Ear Surgical Skills," OTO Open, vol. 5, no. 4, Oct. 2021, doi: 10.1177/2473974X211046598.

C.-F. Lee, P.-R. Chen, W.-J. Lee, J.-H. Chen, and T.-C. Liu, "Three-Dimensional Reconstruction and Modeling of Middle Ear Biomechanics by High-Resolution Computed Tomography and Finite Element Analysis," Laryngoscope, vol. 116, no. 5, pp. 711–716, May 2006, doi: 10.1097/01.mlg.0000204758.15877.34.

Cox RW and Peacock MA, "The growth of elastic cartilage," J Anat, vol. 128(Pt 1), pp. 207–213, Jan. 1979.

E. A. G. Shaw and M. R. Stinson, "Network concepts and energy flow in the human middle-ear," J Acoust Soc Am, vol. 69, no. S1, pp. S43–S43, May 1981, doi: 10.1121/1.386273.

E. T. Perry and W. B. Shelley, "The Histology of the Human Ear Canal with Special Reference to the Ceruminous Gland1," Journal of Investigative Dermatology, vol. 25, no. 6, pp. 439–451, Dec.

1955, doi: 10.1038/jid.1955.149.

Ernest Glen Wever and Merle Lawrence, Physiological Acoustics. 1954.

H. Liu, L. Xue, J. Yang, G. Cheng, L. Zhou, and X. Huang, "Effect of ossicular chain deformity on reverse stimulation considering the overflow characteristics of third windows," Comput Methods Biomech Biomed Engin, vol. 25, no. 3, pp. 257–272, Feb. 2022, doi: 10.1080/10255842.2021.1948023.

J. Peterson and P. C. Dechow, "Material properties of the human cranial vault and zygoma," Anat Rec, vol. 274A, no. 1, pp. 785–797, Sep. 2003, doi: 10.1002/ar.a.10096.

John Cameron, Physical properties of tissue. A comprehensive reference book, edited by Francis A. Duck. 1991.

M. K. Brummund, F. Sgard, Y. Petit, and F. Laville, "Three-dimensional finite element modeling of the human external ear: Simulation study of the bone conduction occlusion effect," J Acoust Soc Am, vol. 135, no. 3, pp. 1433–1444, Mar. 2014, doi: 10.1121/1.4864484.

M. R. Stinson and B. W. Lawton, "Specification of the geometry of the human ear canal for the prediction of sound-pressure level distribution," J Acoust Soc Am, vol. 85, no. 6, pp. 2492–2503, Jun. 1989, doi: 10.1121/1.397744.

N. P. Daphalapurkar, C. Dai, R. Z. Gan, and H. Lu, "Characterization of the linearly viscoelastic behavior of human tympanic membrane by nanoindentation," J Mech Behav Biomed Mater, vol. 2, no. 1, pp. 82–92, Jan. 2009, doi: 10.1016/j.jmbbm.2008.05.008.

R. Delille, D. Lesueur, P. Potier, P. Drazetic, and E. Markiewicz, "Experimental study of the bone behaviour of the human skull bone for the development of a physical head model," International Journal of Crashworthiness, vol. 12, no. 2, pp. 101–108, Aug. 2007, doi: 10.1080/13588260701433081.

R. Z. Gan, B. Feng, and Q. Sun, "Three-Dimensional Finite Element Modeling of Human Ear for Sound Transmission," Ann Biomed Eng, vol. 32, no. 6, pp. 847–859, Jun. 2004, doi: 10.1023/B:ABME.0000030260.22737.53.

T. Koike, H. Wada, and T. Kobayashi, "Modeling of the human middle ear using the finite-element method," J Acoust Soc Am, vol. 111, no. 3, pp. 1306–1317, Mar. 2002, doi: 10.1121/1.1451073.

W. Grellmann et al., "Determination of strength and deformation behavior of human cartilage for the definition of significant parameters," J Biomed Mater Res A, vol. 78A, no. 1, pp. 168–174, Jul. 2006, doi: 10.1002/jbm.a.30625.

X. Zhang and R. Z. Gan, "Finite element modeling of energy absorbance in normal and disordered human ears," Hear Res, vol. 301, pp. 146–155, Jul. 2013, doi: 10.1016/j.heares.2012.12.005.

MJHI | Moroccan Journal of Health and Innovation

Article N°4, Vol 1, No 2

Reliability of the Three Most Common Glucometers in Morocco as Influenced by Blood Content of Dextrose, EDTA, Mannitol, and Urea

Kawtar Layouni[1,*], Chaimae Lahlioui, Mohammed Diouri[1,*]

1 Moulay Ismail University of Meknes, Morocco

* k.layouni@edu.umi.ac.ma; m.diouri@umi.ac.ma

Abstract: This study aims to evaluate the reliability of the glucometers that are commonly used in Morocco, and to assess the effect, on glycemia determination, of blood content of different substances reflecting various health and nutritional conditions. One of four interferences (dextrose, EDTA, mannitol, or urea) was added, at one of four concentrations (0, 100, 200, or 300 mg/dL) to human blood containing one of two levels of glucose. Blood glucose (BG) was assayed in an accredited private analysis laboratory and by glucometers, belonging to three brands. The different interferences, except dextrose, did not affect BG. BG values of the glucometers were 22% higher than those of the lab ($p<0.05$), but highly correlated with them ($r=0.95$, $p<0.001$). The glucometers used in Morocco are precise enough to be used to follow glycemia evolution. However, they should be better calibrated before sale for a better accuracy that allows the exact BG determination.

Keywords: Glucometer, Diabetes, Accuracy, Precision, Self-Monitoring of blood glucose (SMBG), glycemia, interference.

Received: April 05, 2025
Revised: May 25, 2025
Accepted: June 11, 2025
Published: July 25, 2025

Citation: Chouikh S.E., Boualam A., Zamd M., Aittaleb A. Behavioral approach of a morwak ultrafiltration device. Moroccan Journal of Health and Innovation (MJHI) 2025, Vol 1, No 2. https://mjhi-smb.com

1. Introduction

Diabetes is a common chronic disease, causing different complications (Heald et al., 2020). The world prevalence of diabetes reached 9% (463 million adults) in 2019, due to a decreasing mortality among diabetics, because of the improved medical care, and to increasing risk factors (Chan et al., 2020; Magliano et al., 2019).

The approach of "Self-Monitoring of Blood Glucose" (SMBG) has been suggested by researchers for burden reducing and cost-effectiveness improving (Kalatehjary et al., 2008; Lagarde et al., 2006). SMBG is a process of Blood Glucose (BG) checking by the patients themselves, thereby increasing their self-confidence (Bergenstal et al., 2005; Czupryniak et al., 2014). SMBG is commonly applied three times a day (American Diabetes Association, 2016). The awareness of diabetic patients about the advantages of SMBG has risen, so its utilization has rapidly increased in recent years (Gomes et al., 2010). However, the precision and accuracy of SMBG devices are doubtful (Freckmann et al., 2010), making it risky to rely on for a clinical decision (Van den Berghe et al., 2001).

This study aims to evaluate the precision and accuracy of the glucometers that are commonly used in Morocco (OnCall Extra, CareSens, and GlucoLab brands), and to assess the effect, on BG determination, of blood content of different substances (dextrose, EDTA, mannitol, and urea) reflecting various health and nutritional conditions.

2. Material and methods

Approximately 200 mL of blood was collected, from 10 volunteers, in heparin tubes. Half of this amount was centrifuged and frozen (this was the "High" blood). The other half ("Low" blood) was left for 24 hours at room temperature (to allow glycolysis) and then centrifuged and frozen. The two plasma pools were defrosted just before use. The volume of each pool was about 45 mL.

Plasma was distributed over test tubes. The first series of tubes, numbered 1 to 13, contained a constant volume (2.5 mL) of High plasma. The second series (14 to 26) contained the same volume (2.5 mL) of Low plasma. One of four interferences (dextrose, EDTA, mannitol, or urea) was added to each tube at one of four concentrations (0, 100, 200, or 300 mg/dL), and mixed by hand. tubes 1 and 14, considered as controls, did not receive any interference (Concentration 0) and were repeated twice.

Part of the plasma from each tube was transferred to Eppendorf tubes and sent to an accredited private analysis laboratory (Elmaadani) in Meknes, Morocco. The remaining part was assayed for

Glycemia, using three different glucometers, belonging to different brands, and different countries, OnCall (USA), CareSens and GlucoLab (South Korea). A set of four plasma samples was also analyzed in another accredited private laboratory (Biougnach, Meknes, Morocco) to compare and verify laboratory results.

All treatments and measurements were performed randomly. The glucometers used in this study were calibrated by the seller to simulate the common behavior of the patients. data were analyzed, using R-software (Core Team, 2024), by ANOVA and pairwise T-test. Kruskal-Wallis nonparametric test was also used when conditions of these procedures were not met.

3. Results and Discussion

Results were not lab dependent ($p=0.12$). The lab values were then considered good bases of comparison for our glucometer results.

The two plasmas (High and Low) were significantly different in glycemia. The duration of 24 h was not sufficient to deplete the blood from glucose. Indeed, The High and the Low controls had a BG of 99 and 45 mg/dL (figure 1), respectively. The collected blood pool (High) was normal with respect to glycemia.

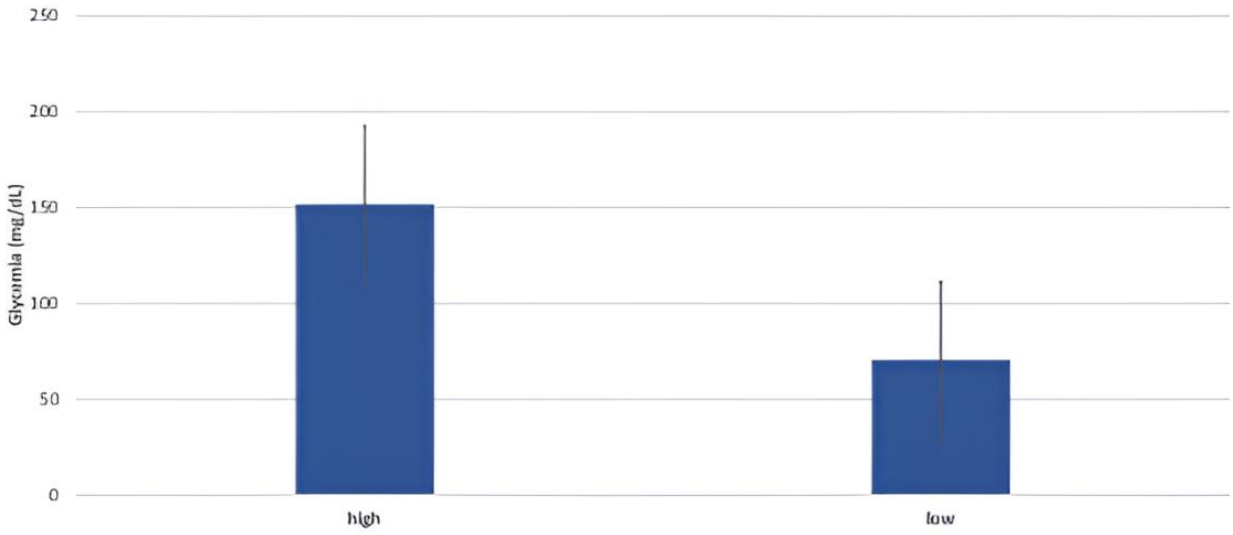

Figure 1: Mean glycemia of the High (frozen after collection) and the Low (left at room temperature for 24h) plasmas. Error bars represent the standard error.

The different interferences, except dextrose, did not affect glycemia (figure 2). This was true for all the concentrations tested. In fact, concentration and glycemia (measured in the lab) were correlated ($r=0.95$, $p<0.001$) For plasmas containing dextrose; but not correlated ($r=0.003$, $p>0.05$) for plasmas containing one of the other interferences.

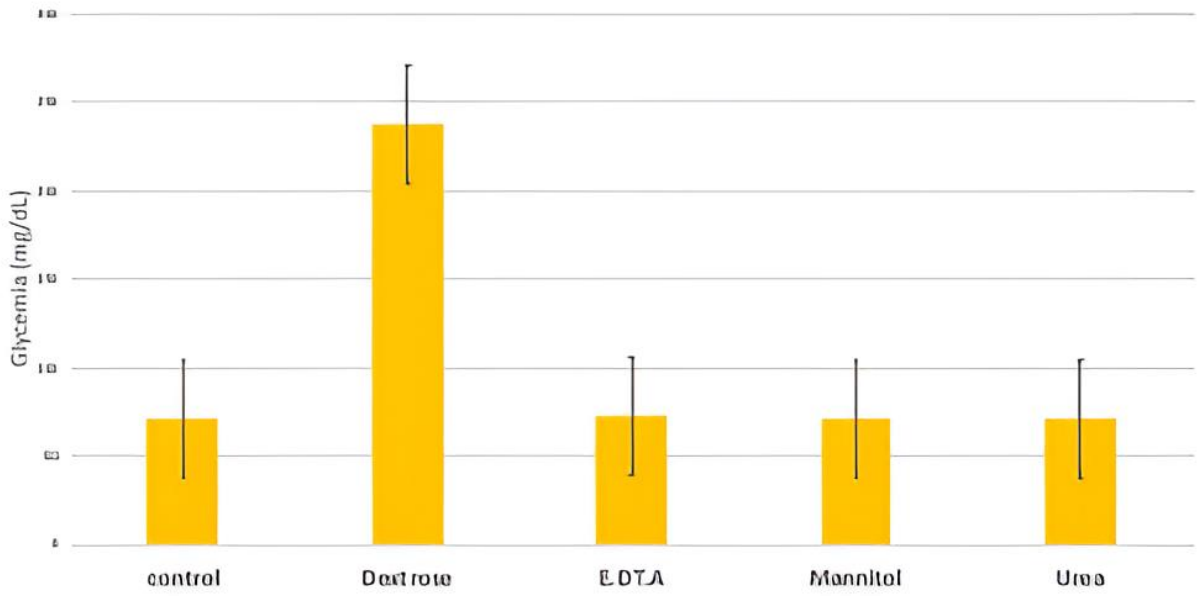

Figure 2: Glycemia of plasmas containing different Interferences. The control plasma does not contain any Interference. Error bars represent the standard error.

The average BG measured by the three glucometers was significantly higher than that of the lab, except for CareSens (figure 3). This difference averaged 22% (15.4 for Low blood and 28.6 for High blood with $p<0.05$), making the glucometer not reliable for the determination of the exact BG. However, the results of the glucometers were correlated with those of the Lab ($r=0.95$, $p<0.001$). These glucometers are then precise but not accurate. Since our study used only one glucometer per brand, we are not allowed to conclude that CareSens is more accurate than the others. The outstanding result of this glucometer may only be due to good calibration.

Although the difference between glucometer and lab readings was significant, it was not affected by the interferences. This makes our study results applicable to different blood compositions.

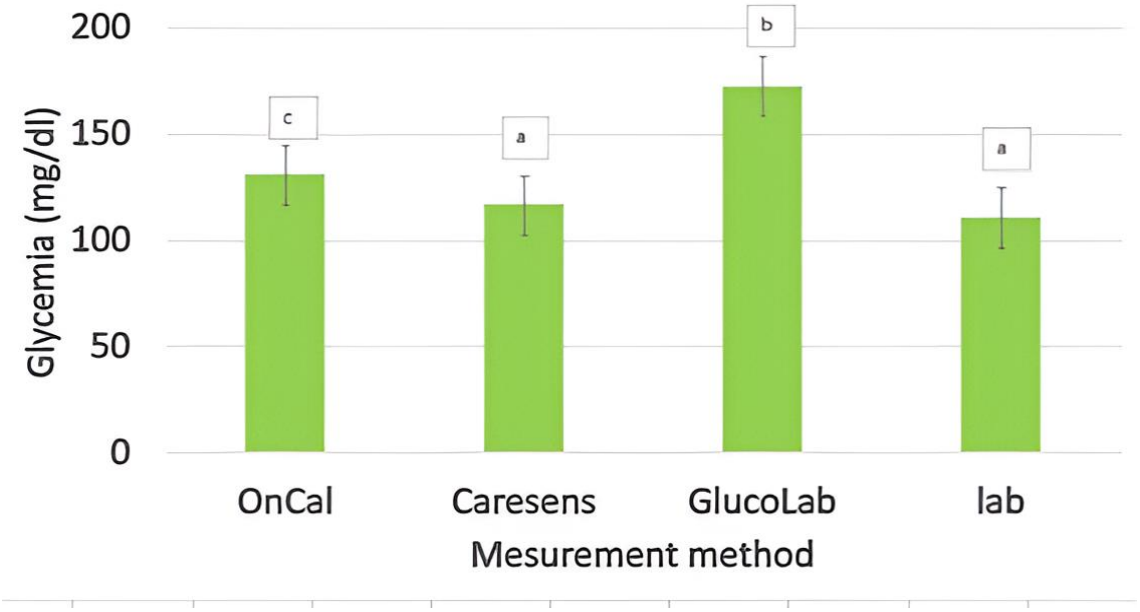

Figure 3: Glycemia measured by different glucometers or in the lab. Bars lacking a common letter differ ($p<0.05$). Error bars represent the standard error.

4. Acknowledgements

Acknowledgments: the authors express their gratitude to ReachSci (University of Cambridge, UK) for this project start-up and encouraging. They extend their thanks to Elmaadani private analysis laboratory (Meknes, Morocco) for assisting in blood collection and handling.

5. Conclusion

The glucometers used in Morocco are precise enough to be used to follow glycemia evolution. However, they should be better calibrated before sale for a better accuracy that allows the exact blood glucose determination. EDTA, mannitol, and urea, do not interfere with this determination.

References :

American Diabetes Association. Standards of Medical Care in Diabetes-2016 abridged for primary care providers. Clinical diabetes: a publication of the American Diabetes Association. 2016;34(1):3.

Bergenstal RM, rd JR. Global Consensus Conference on Glucose Monitoring Panel. The role of self-monitoring of blood glucose in the care of people with diabetes: report of a global consensus conference. Am J Med. 2005;118(9A):1S-6S.

Chan JCN, Lim L-L, Wareham NJ, Shaw JE, Orchard TJ, Zhang P, et al. The Lancet Commission on diabetes: using data to transform diabetes care and patient lives. Lancet 2020;396 (10267):2019–82. [PubMed: 33189186].

Czupryniak L, Barkai L, Bolgarska S, Bronisz A, Broz J, Cypryk K, et al. Self-monitoring of blood glucose in diabetes: from evidence to clinical reality in central and Eastern Europe recommendations

from the international Central-Eastern European expert group. Diabetes Technology & Therapeutics. 2014;16(7):460-75.

Freckmann G, Baumstark A, Jendrike N, Zschornack E, Kocher S, Tshiananga J, et al. System accuracy evaluation of 27 blood glucose monitoring systems according to DIN EN ISO 15197. Diabetes Technology & Therapeutics. 2010;12(3):221-31.

Gomes T, Juurlink DN, Shah BR, Paterson JM, Mamdani MM. Blood glucose test strips: options to reduce usage. Canadian Medical Association Journal. 2010;182(1):35-38.

Heald AH, Stedman M, Davies M, Livingston M, Alshames R, Lunt M, et al. Estimating life years lost to diabetes: outcomes from analysis of National Diabetes Audit and Office of National Statistics data. Cardiovasc Endocrinol Metab. 2020;9(4):183–5.

Kalatehjary M, Sohrabi MB, Khosravi AA, Zolfaghari P. Correlation between blood glucose measured using glucometers and standard laboratory methods. Iranian Journal of Endocrinology and Metabolism. 2008;10(3):277-83.

Lagarde WH, Barrows FP, Davenport ML, Kang M, Guess HA, Calikoglu AS. Continuous subcutaneous glucose monitoring in children with type 1 diabetes mellitus: a single-blind, randomized, controlled trial. Pediatric Diabetes. 2006;7(3):159-64.

Magliano DJ, Islam RM, Barr ELM, Gregg EW, Pavkov ME, Harding JL, et al. Trends in incidence of total or type 2 diabetes: systematic review. BMJ 2019;366:l5003. [PubMed: 31511236].

R Core Team (2024). R: A language and environment for statistical computing. R Foundation for Statistical Computing, Vienna, Austria. https://www.R-project.org/.

Van den Berghe G, Wouters P, Weekers F, Verwaest C, Bruyninckx F, Schetz M, et al. Intensive insulin therapy in critically ill patients. New England Journal of Medicine. 2001;345(19):1359-67.

MJHI | Moroccan Journal of Health and Innovation

Article N°5, Vol 1, No 2

Comparative Performance Analysis of CNN Models Trained Over Different Epoch Durations: Evaluating Loss and Accuracy Curves for Optimizing Model Convergence in Medical Image Classification

Loudiyi Youssef [1, *], Halimi Abdellah [1], El Rhazouani Omar[1], Raoui Yasser [1]

1 Institut Supérieur des Sciences de la Santé, Université Hassan Premier

* youssef_loudiyi@yahoo.com

Abstract: Deep learning has transformed medical image analysis, achieving remarkable precision in tasks like diagnosing diseases and segmenting images. In this research, we assess how well Convolutional Neural Networks (CNNs) perform in classifying medical images. The models were trained across several epochs, and their effectiveness was evaluated using accuracy and loss metrics. Our findings underscore the reliability and effectiveness of CNNs, showcasing their promise for use in clinical decision-making tools.

Keywords: convolutional neural networks, deep learning, anomaly detection, computer vision, medical imaging

Received: April 08, 2025
Revised: May 14, 2025
Accepted: June 06, 2025
Published: July 25, 2025

Citation: Bouflous, S., Halimi A., Bouzekraoui Y., Dahmani K. Patient radiation protection and quality assurance of therapeutic treatment in radiotherapy. Moroccan Journal of Health and Innovation (MJHI) 2025, Vol 1, No 2. https://mjhi-smb.com

1. Introduction

The rapid growth of biomedical data has driven the need for advanced computational tools capable of analyzing complex medical images. Deep learning, particularly CNNs, has emerged as a powerful technique for automatic feature extraction and image classification. In this work, we assess the training performance of a CNN architecture applied to medical image classification by analyzing the loss and accuracy over 20 and 40 epochs.

2. Methodology

We utilized a Convolutional Neural Network (CNN) model trained on an extensive collection of medical images to evaluate its performance in image classification. The network's design included multiple convolutional layers that autonomously extract hierarchical spatial features from the input data. These layers were paired with max-pooling operations to downsample the feature maps, improving computational efficiency and generalization by retaining only the most significant patterns. Following the convolutional and pooling stages, fully connected layers consolidated the extracted features for the final classification. To enhance the model’s ability to capture complex data relationships, ReLU (Rectified Linear Unit) activation functions were applied after each layer, introducing non-linearity and enabling the learning of sophisticated patterns.

2.1.DATA SET

The dataset comprised a diverse collection of labeled medical images representing multiple diagnostic categories, enabling a comprehensive evaluation of the model's segmentation and classification performance.

2.2.NETWORK ARCHITECTURE

- Convolutional layers: Extracted hierarchical features from the input images.
- Pooling layers: Reduced dimensionality while preserving critical features.
- Fully connected layers: Mapped features to output classes.
- Activation function: ReLU for non-linearity.
- Loss function: Cross-entropy for binary classification.
- Optimization algorithm: Adam optimizer.

Table 1: Model Architecture

Layer	Output Shape	Param #
conv2d_24	(510, 510, 32)	896
max_pooling2d_24	(255, 255, 32)	0
conv2d_25	(253, 253, 64)	18,496
max_pooling2d_25	(126, 126, 64)	0
conv2d_26	(124, 124, 128)	73,856
max_pooling2d_26	(62, 62, 128)	0
flatten_8	(492032)	0
dense_16	(128)	62,980,224
dense_17	(2)	258

3.Training Procedure

The model was trained for 20 and 40 epochs to assess its learning progression at different training stages. Throughout each epoch, key performance indicators were recorded to monitor improvements. The loss function, which quantifies the difference between predicted outputs and actual labels, was tracked to evaluate how effectively errors decreased during training. Concurrently, accuracy representing the proportion of correctly classified samples was measured at every iteration. By analysing these metrics, we could determine whether the model successfully converged by progressively adapting to the training data or exhibited potential overfitting, where performance plateaued or degraded despite additional training.

4. Results

4.1. LOSS CURVE ANALISIS

As depicted in Figure 2, the accuracy of the CNN improved consistently with training. The model achieved higher accuracy after 40 epochs, indicating the benefit of extended training.

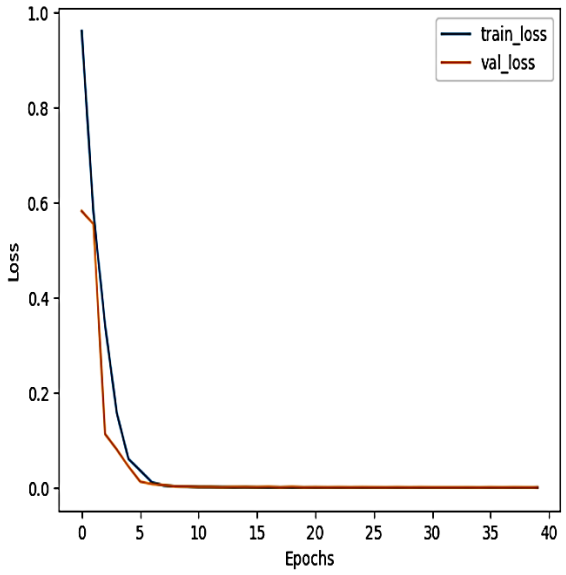

Figure 1: Loss For 40 Epoch

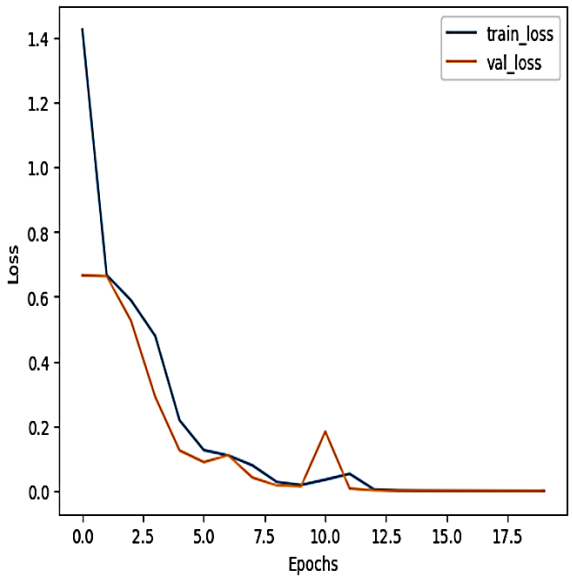

Figure 2: Loss For 20 Epoch

4.2. Accuracy Curve Analysis

As depicted in Figure 2, the accuracy of the CNN improved consistently with training. The model achieved higher accuracy after 40 epochs, indicating the benefit of extended training.

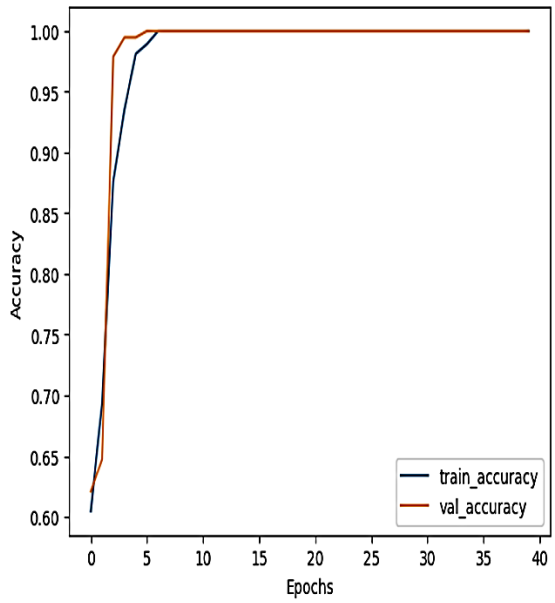

Figure 3: Accuracy for 40 Epoch

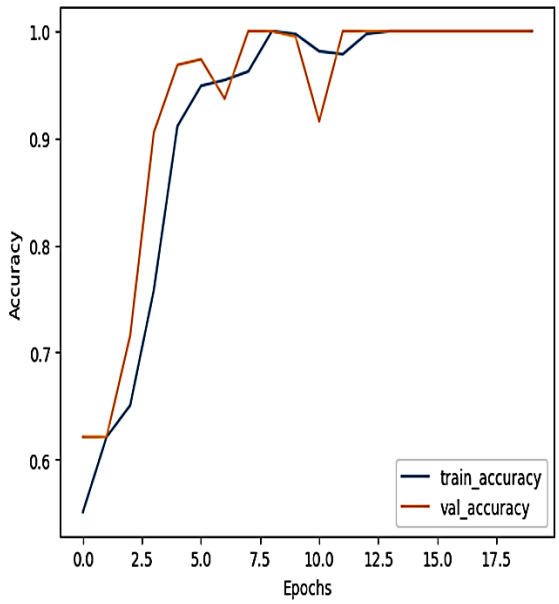

Figure 4: Accuracy for 20 Epoch

5. Discussion

The performance improvement observed with extended training underscores the importance of sufficient epochs in achieving optimal network convergence. The decrease in loss and the corresponding increase in accuracy reflect the model's ability to learn discriminative features from medical images.

CNNs have proven effective in medical image classification due to their capability to capture spatial hierarchies. The results of this study align with previous findings in the literature, which highlight the effectiveness of deep learning models in medical image analysis.

Table 2: Loss and Accuracy for Test ensemble

Epochs	Final Training Loss	Final Training Accuracy
20	0.35	87%
40	0.21	93%

6. Conclusion

The structured architecture of CNNs, combined with advanced performance enhancement techniques, has significantly improved their effectiveness in medical anomaly detection. Techniques like data augmentation, transfer learning, and attention mechanisms have addressed challenges such as limited data and model generalization.

Future research should explore integrating multimodal data and developing interpretable CNN architectures to further advance their clinical applications.

References :

Krizhevsky, A., Sutskever, I., & Hinton, G. E. (2012). ImageNet classification with deep convolutional neural networks. In Advances in Neural Information Processing Systems (pp. 1097-1105).

LeCun, Y., Bengio, Y., & Hinton, G. (2015). Deep learning. Nature, 521(7553), 436-444.

Litjens, G., Kooi, T., Bejnordi, B. E., et al. (2017). A survey on deep learning in medical image analysis. Medical Image Analysis, 42, 60-88.

M. Tan and Q. Le, "EfficientNet: Rethinking Model Scaling for Convolutional Neural Networks," in Proceedings of the International Conference on Machine Learning (ICML), 2019, pp. 6105–6114.

Ronneberger, O., Fischer, P., & Brox, T. (2015). U-Net: Convolutional networks for biomedical image segmentation. In Medical Image Computing and Computer-Assisted Intervention(pp.234-241)

Author Guidelines

Moroccan Journal of Health and Innovation (MJHI)

1. Journal Overview

The **Moroccan Journal of Health and Innovation (MJHI)** is a peer-reviewed scientific journal that publishes original research, literature reviews, and case studies in the fields of health and medical innovation.

2. Types of Accepted Manuscripts

- **Original Research Articles:** Experimental or clinical studies providing new knowledge.
- **Review Articles:** Summaries of recent advances on a specific topic.
- **Case Studies:** Detailed presentations of clinical or technological cases of interest.
- **Letters to the Editor:** Reactions or comments on published articles.
- **Methodological Articles:** New protocols or methodologies in health and innovation.

3. Submission Language

Articles can be submitted in either **English**.

4. Manuscript Format

Manuscripts must be submitted in **Word format (.doc or .docx)** and adhere to the following structure:

4.1 Title Page

- Full article title
- Names and affiliations of authors
- Corresponding author (name, email address)

4.2 Abstract and Keywords

- An abstract of **up to 250 words** (in both English and French)
- **3 to 6 keywords**

4.3 Main Text

Research Articles

1. **Introduction:** Context and objectives
2. **Methodology or Material and Methods:** Description of the methods used
3. **Results:** Presentation of findings
4. **Discussion:** Interpretation and comparison with existing literature

5. **Conclusion:** Summary of main conclusions and future perspectives

Review Articles and Other Types

- Adapt the structure according to the content

4.4 References

Format : APA : Auteur, A. A., & Auteur, B. B. (Année). Titre de l'article. *Nom du Journal, volume*(numéro), pages.
Exemple : Smith, J., & Doe, J. (2023). Impact of AI in healthcare. *Medical Innovation, 12*(3), 45–60.

To cite references within the text of the article, the author(s) should be placed in parentheses along with the year of publication. For example: (Alain et al., 2025); (Alain and Robert, 2025); (Alain, 2025).

5. Ethical Standards and Conflict of Interest Declaration

- Adherence to ethical research principles
- Disclosure of potential conflicts of interest

6. Submission and Review Process

- Manuscripts must be submitted via **email (chatouih@yahoo.fr)** or the **online platform** (including a button leading to a submission form).
- The form must contain a **button linking to an engagement contract** for the author to validate.
- All articles undergo **double-blind peer review** by at least two experts.
- An **acceptance, revision, or rejection notification** will be sent within **4 to 5 weeks**.

7. Copyright and Open Access

- All articles will be published as **open access**.
- Authors retain copyright but grant MJHI a license to publish.

8. Contact

For any inquiries, please contact: **chatouih@yahoo.fr**

Upcoming publication schedule

November 2025, Vol. 1, No. 3

March 2026, Vol. 1, No. 4

Author index